Ultrafast Laser-Pump XAFS- Probe Measurements of Solvated Transition Metal Coordination Complexes Using a Table-Top X-ray Source

Workshop on Time-Domain Science Using X-ray Techniques
August 2004

C. Rose-Petruck
Department of Chemistry,
Brown University, Providence, R.I.

www.rosepetruck.chem.brown.edu

Outline

- High-brightness, tabletop x-ray sources
  - High-average power lasers for x-ray generation
  - Ultrafast x-ray sources and x-ray optics
- Structural deformations of solvated $Fe(CO)_5$
  - Density Functional Theory Calculations
  - FTIR measurements and conformer distribution
  - XAFS measurements and molecular structure
- Ultrafast XANES
  - Expected ligand substitution dynamics of $Fe(CO)_5$
  - UXAFS features of $Fe(CN)_5^{4-}$
  - Example: Simulation of ultrafast x-ray diffraction
- Future performances of laser plasma sources

Outline

- **High-brightness, tabletop x-ray sources**
  - **High-average power lasers for x-ray generation**
  - **Ultrafast x-ray sources and x-ray optics**
- Structural deformations of solvated $Fe(CO)_5$
  - Density Functional Theory Calculations
  - FTIR measurements and conformer distribution
  - XAFS measurements and molecular structure
- Ultrafast XANES
  - Expected ligand substitution dynamics of $Fe(CO)_5$
  - UXAFS features of $Fe(CN)_5^{4-}$
  - Example: Simulation of ultrafast x-ray diffraction
- Future performances of laser plasma sources

Ultrafast laser for laboratory-based plasma x-ray sources

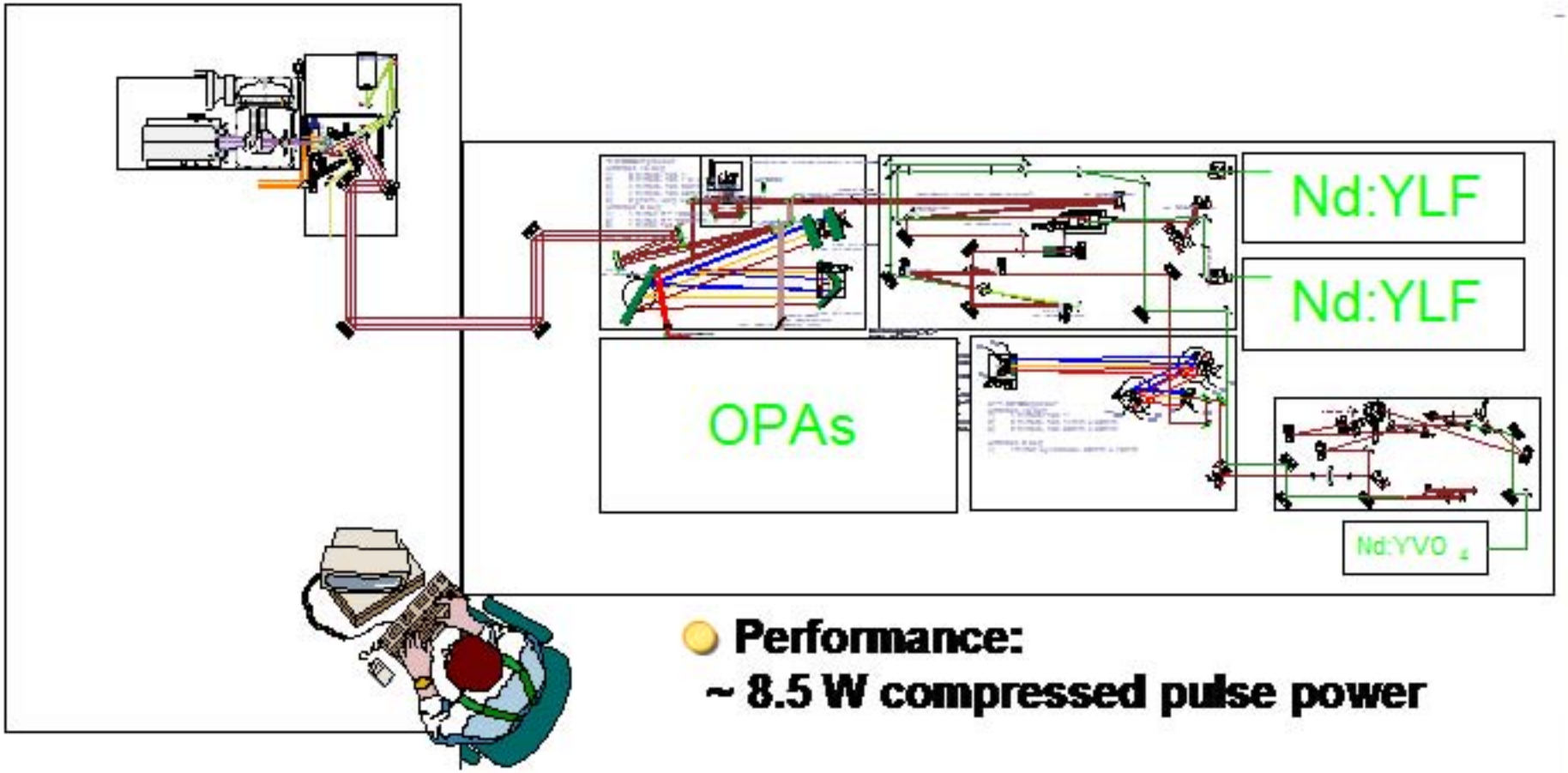

- **Performance:**
  ~ 8.5 W compressed pulse power

Ultrafast x-ray pulses at 2 kHz repetition rate

Laser pulse:	800 nm, 40 fs, 4 mJ, 2KHz
Average laser power before compressor :	13–15W
Average compressed power:	8.5W
Laser intensity:	~ 10^{16} W/cm^2
X-ray flux @ 8keV:	10^{10} photons / (s 4π sr)

Y. Jiang, T. Lee, W. Li, G. Kelwaroo and C. Rose-Petruck, Opt. Lett. 27 (2001)
Y. Jiang, T. Lee and C. Rose-Petruck, J. Opt. Soc. Am. B 20, (2003)

X-ray emission spectrum of 2-kHz source

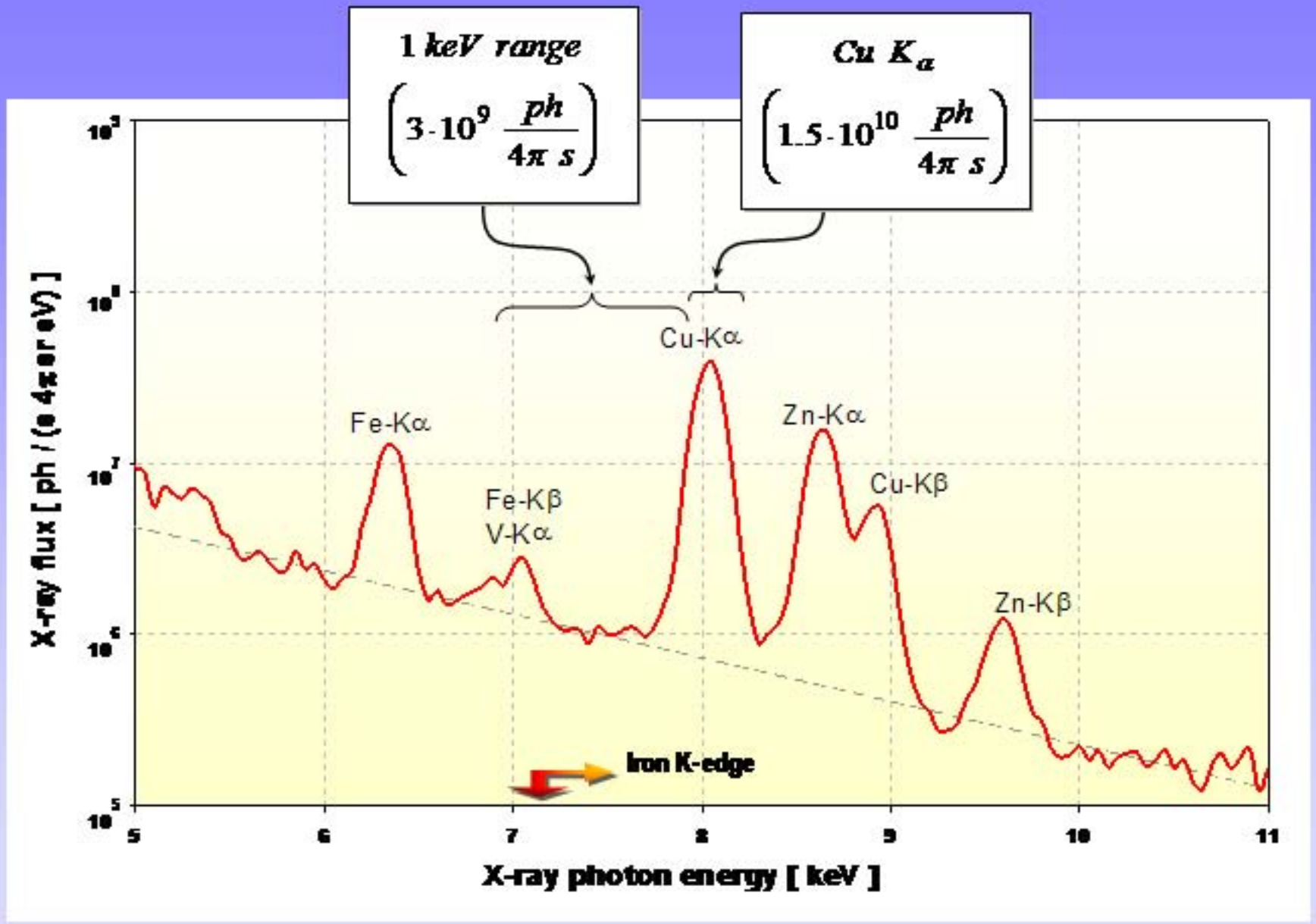

Ultrafast laser-driven XAFS spectrometer

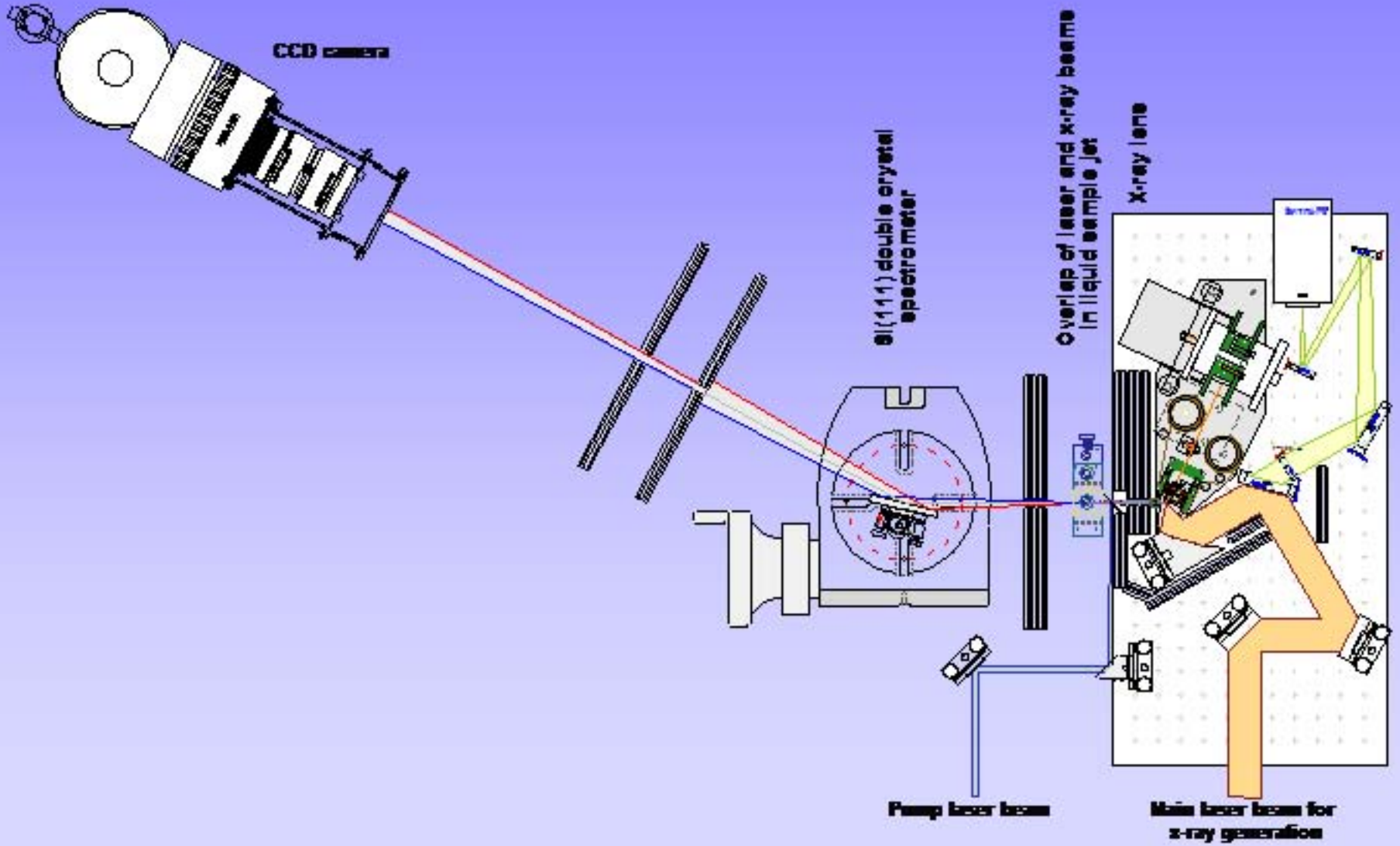

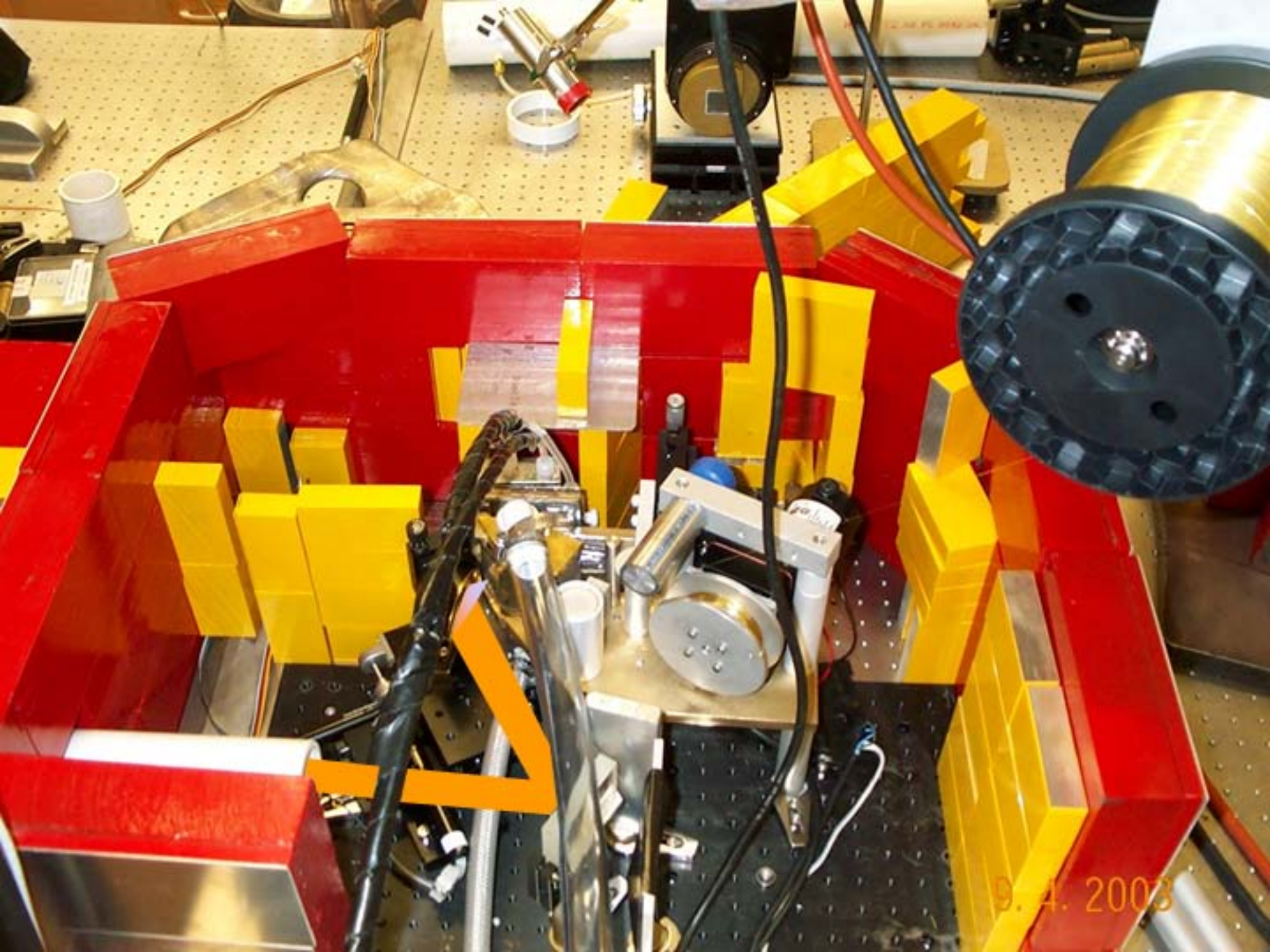
9. 4. 2003

Wire source

X-ray lens mounted on 3D Translation Stage

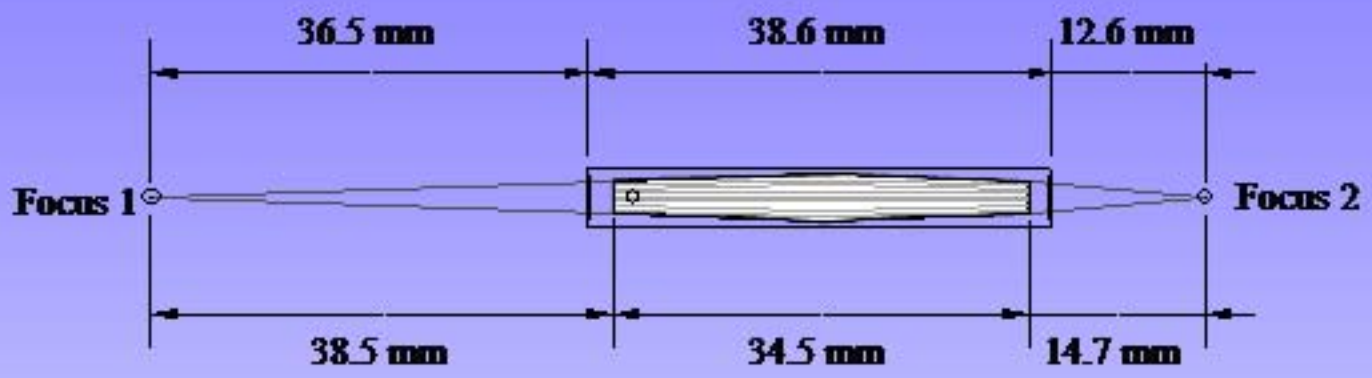

	Focus 1	Focus 2
Focal Length	38.5±0.5 mm	14.7±0.1 mm
Diameter	1.7 mm	1.4 mm
ϕ	0.044 rad / 2.5°	0.095 rad / 5.4°

Laser plasma x-radiation imaged into sample by x-ray lens

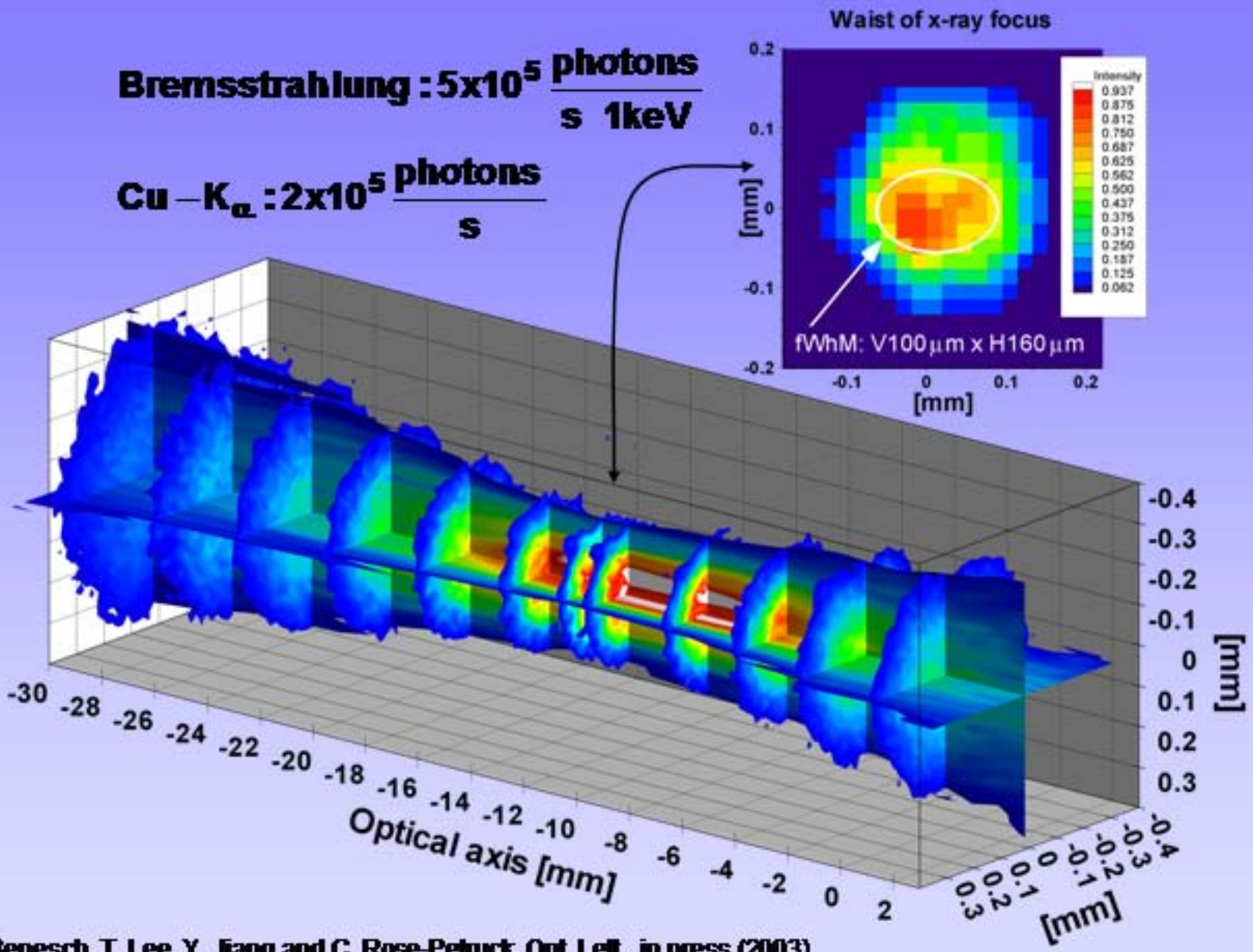

F. Benesch, T. Lee, Y. Jiang and C. Rose-Petruck, Opt. Lett., in press (2003)

Low-resolution x-ray spectrum after x-ray lens

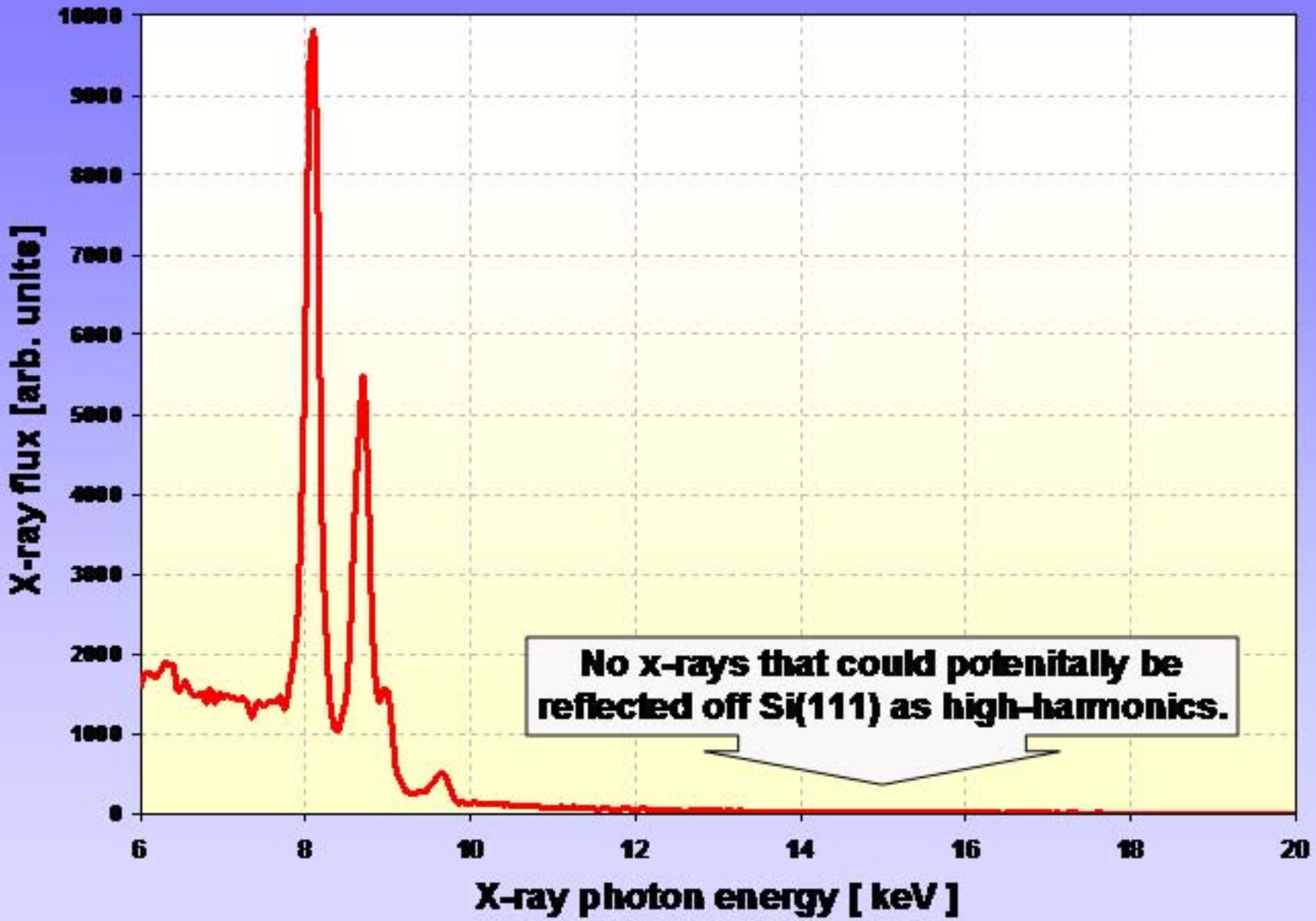

$Fe(CO)_5$

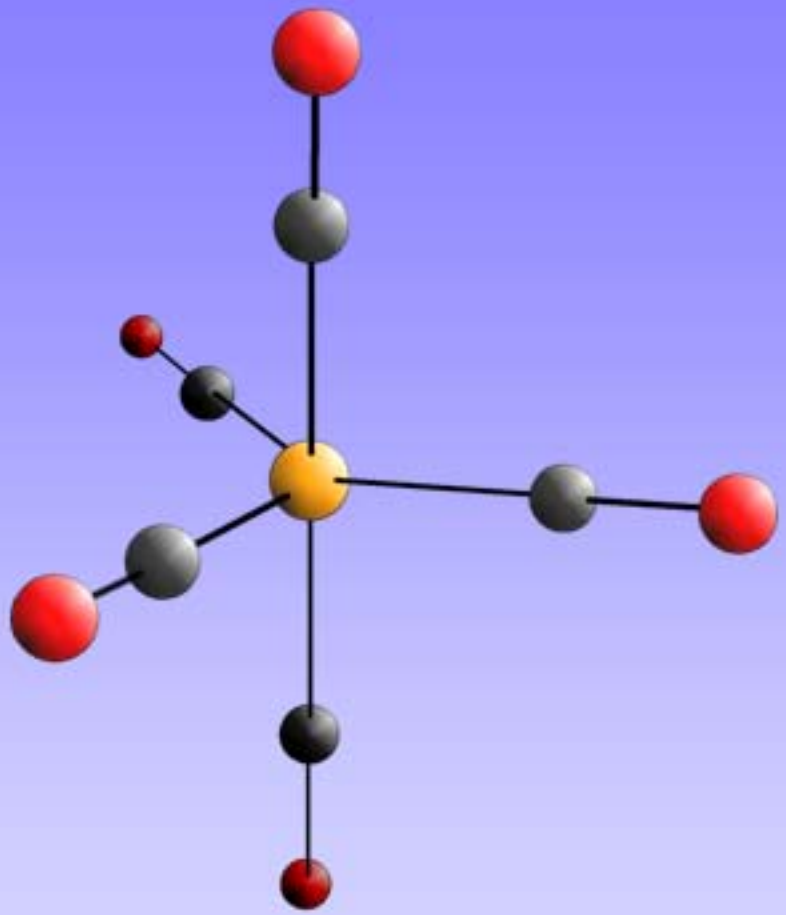

D_{3h}

Independent XAFS parameters

$$N_I = \frac{2\Delta k\,\Delta R}{\pi} + 2$$

Stern, E. A. Phys. Rev. B 48, 9825-7 (1993)

$\Delta k = 6.5\ \text{Å}^{-1}$, $\Delta R = 1.2\ \text{Å} \Rightarrow N_I = 7$

$R(Fe-O)$,

$\sigma^2(Fe-O)$

$R(Fe-C)$,

$\sigma^2(Fe-C)$,

S_0^2, E_0.

Electron density isosurface of $Fe(CO)_5$ in 10 Benzene

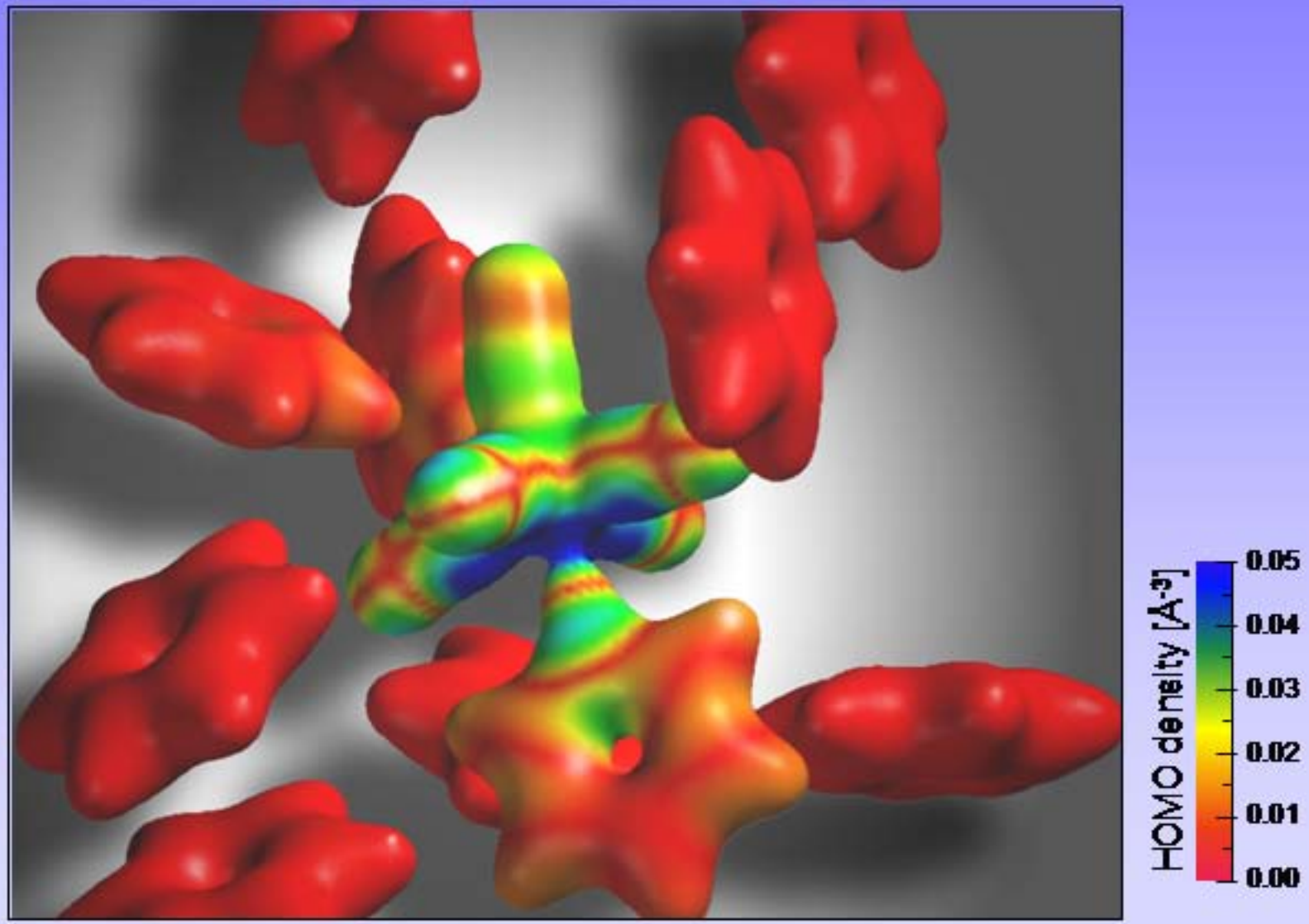

Outline

- High-brightness, tabletop x-ray sources
  - High-average power lasers for x-ray generation
  - Ultrafast x-ray sources and x-ray optics
- **Structural deformations of solvated $Fe(CO)_5$**
  - **Density Functional Theory Calculations**
  - **FTIR measurements and conformer distribution**
  - **XAFS measurements and molecular structure**
- Ultrafast XANES
  - Expected ligand substitution dynamics of $Fe(CO)_5$
  - UXAFS features of $Fe(CN)_5^{4-}$
  - Example: Simulation of ultrafast x-ray diffraction
- Future performances of laser plasma sources

Normal vibrational modes of $Fe(CO)_5$

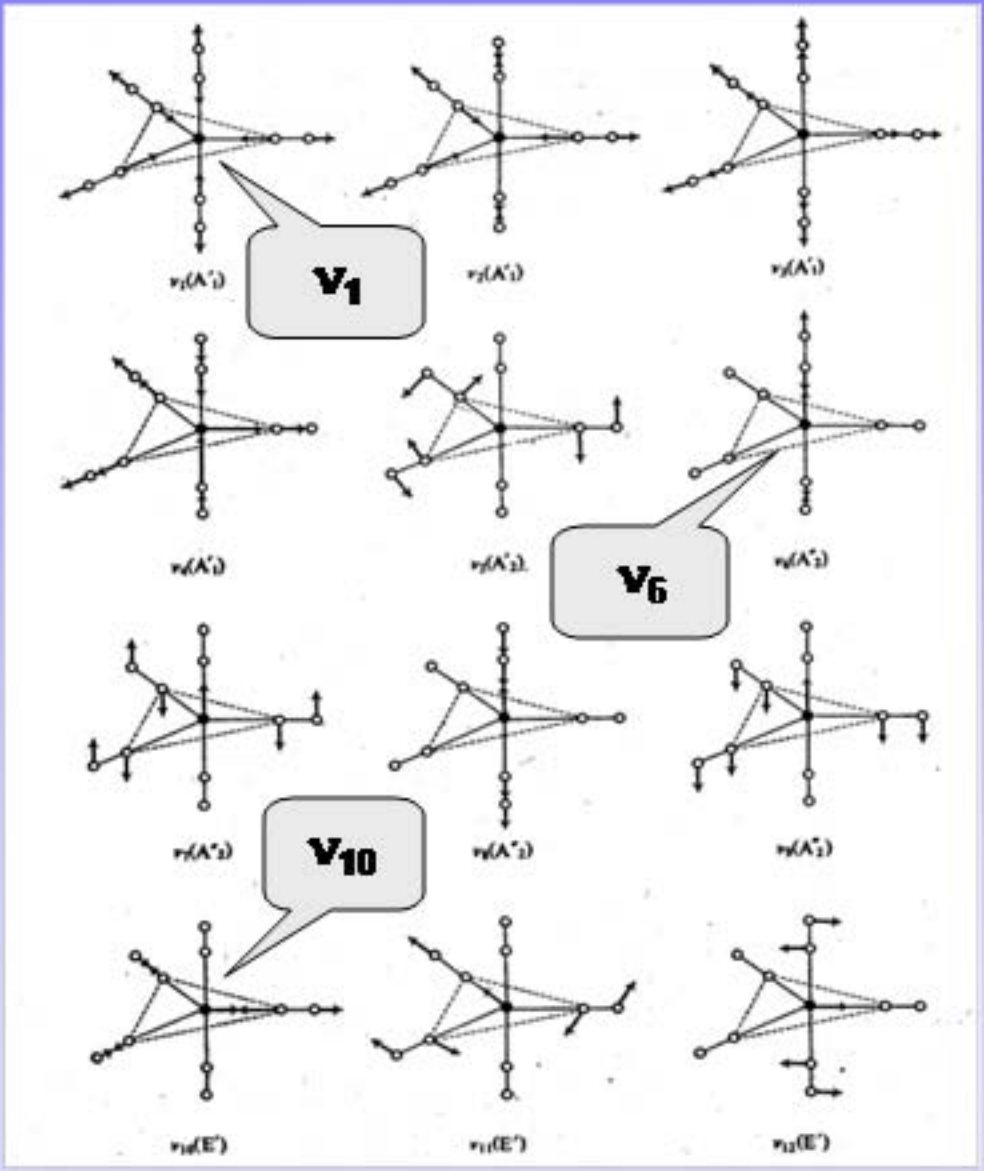

18 fundamental vibrations

- Two C-O stretching modes, $\nu_6(A''_2)$ and $\nu_{10}(E')$ are IR active
- The C-O stretching modes, $\nu_1(A'_1)$ is Raman active

Reproduced from Metal-Ligand and Related vibrations, D. M. Adams(1968)

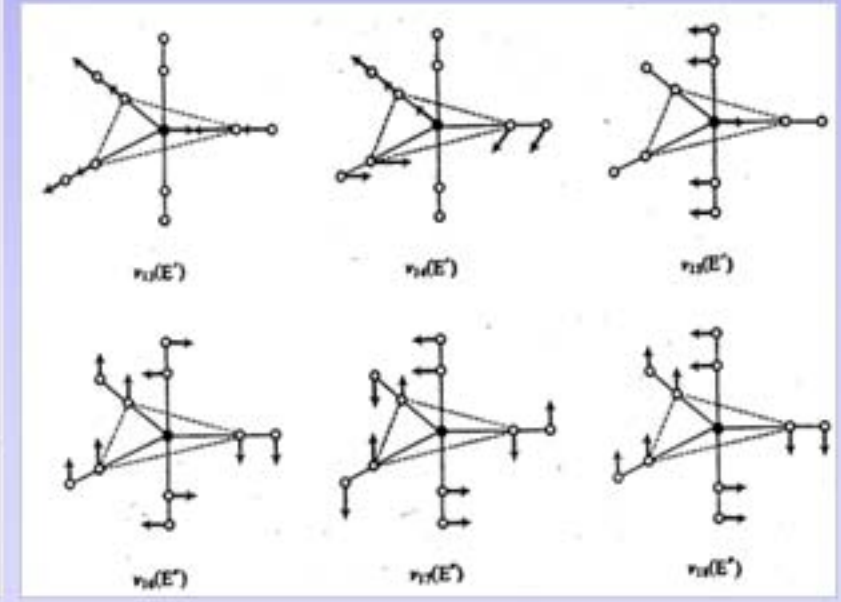

ν_1-IR absorption spectra of IPC in fluorinated benzenes

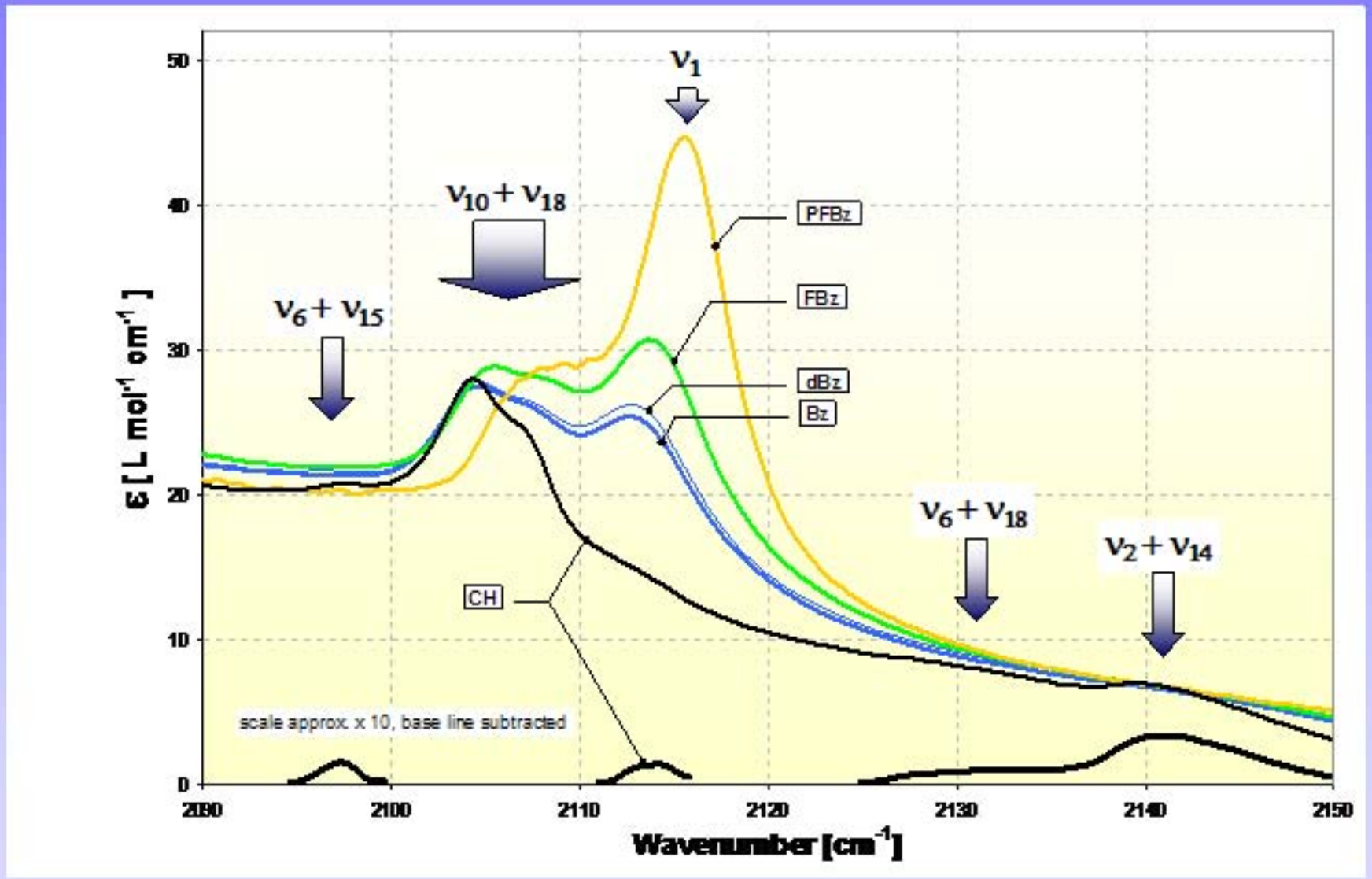

Berry pseudorotation

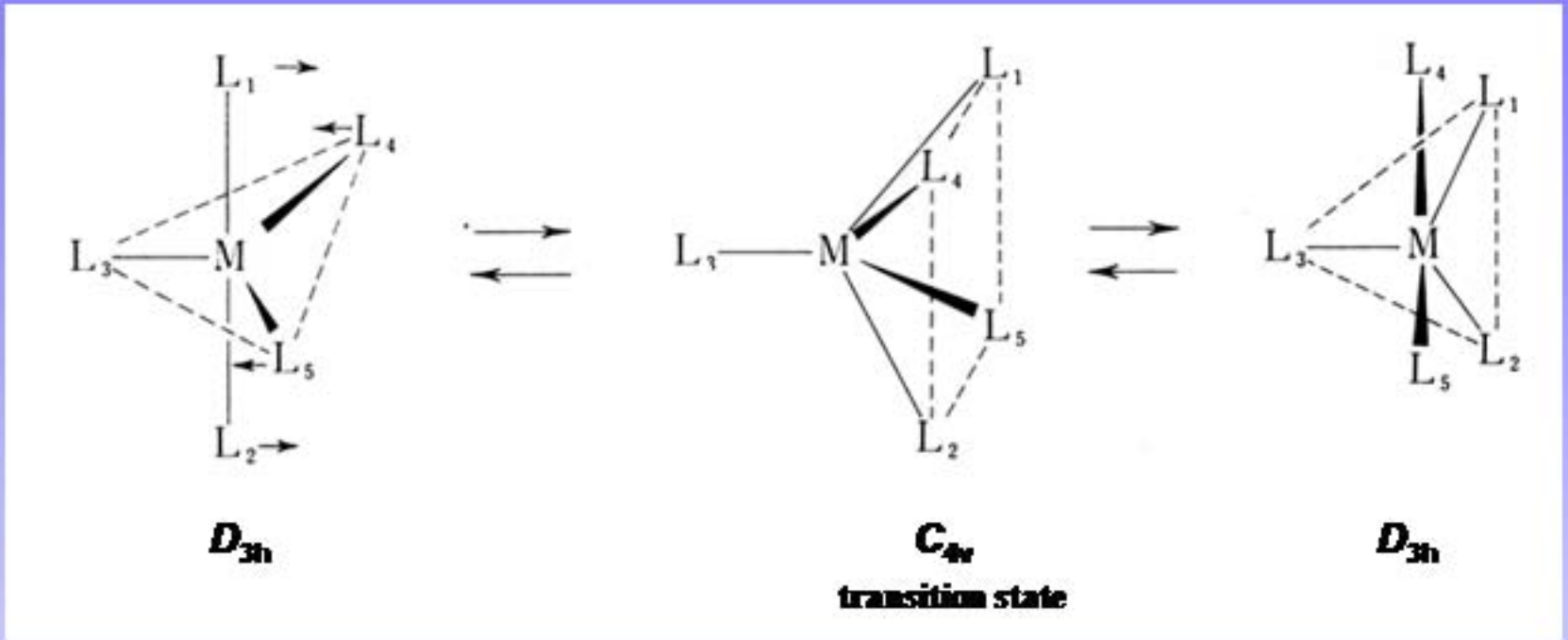

The energy barrier between C_{4v} and D_{3h} is between 1 kcal/mol (NMR) [1] and 2.3 kcal/mol (theoretical calculations) [2,3].

1. Spiess, H.W.; Grosescu, R.; Haeberlen, U. Chem. Phys. 1974, 6, 226
2. J. H. Jang, J. G. Lee, and H. Lee, J. Phys. Chem. A 1998, 102, 5298-5304
3. Demuynck, J.; Strich, A.; and Veillard, A., Nouveau J. de Chim., 1977, 1(3), 217-228

IPC-Bz structures at various solute-solvent distances

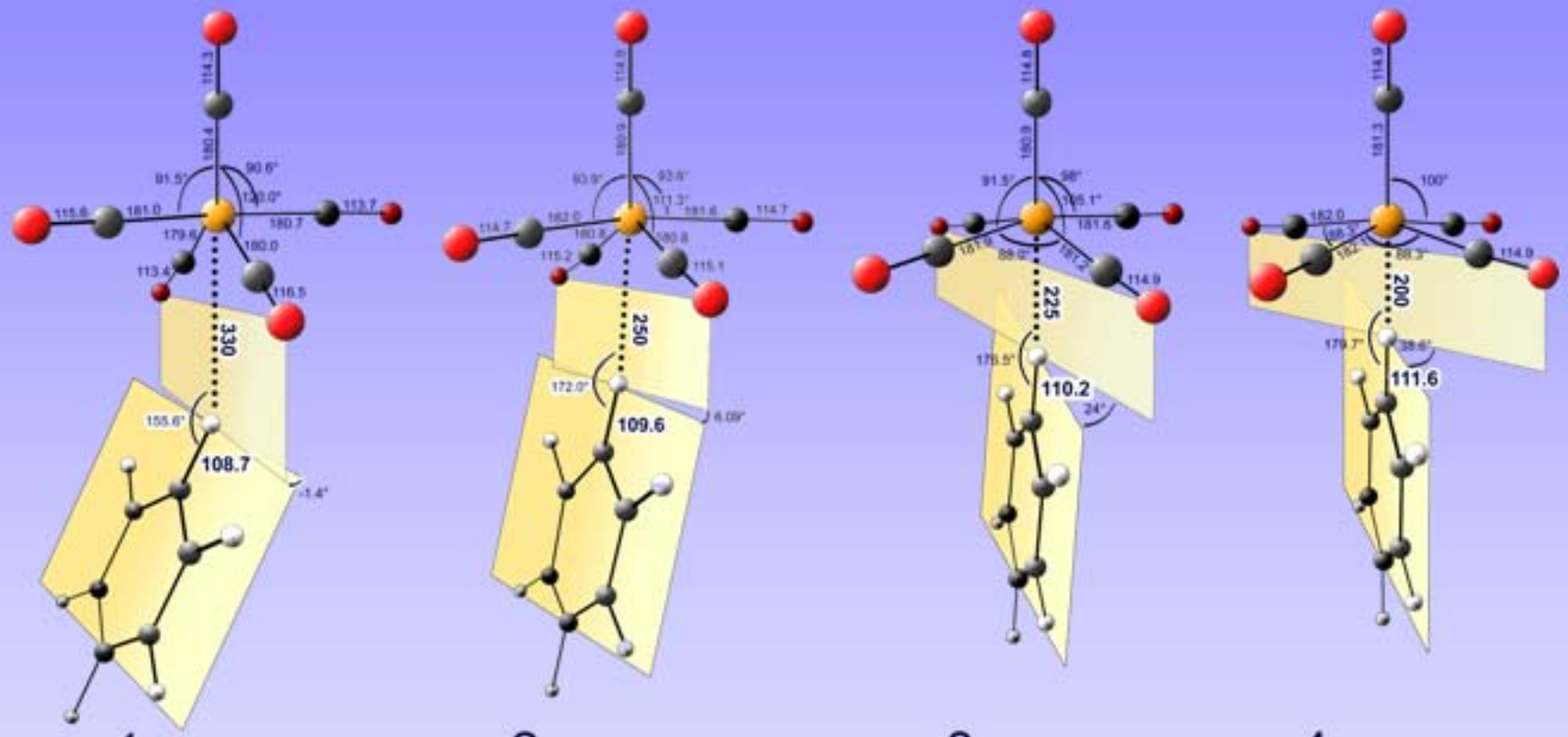

1 (IPC: ~D_{3h}) 2 (IPC: C_{2v}) 3 (IPC: C_{2v}) 4 (IPC: ~C_{4v})

Conformer data of IPC in fluorinated benzenes

		From combined FTIR and DFT data		From temperature- dependent FTIR data	
Solvent	Equilibrium IPC···Solvent distance (pm)	Average C_{2v}-poulation at average IPC···S distance	$\Delta_{conf}G$ (kJ /mol)	Average C_{2v}-population at average IPC···S distance	$\Delta_{conf}G$ (kJ /mol)
CH	330	16.0%	4.1		
Bz	254	65.3%	-1.6	61.6%	-1.17
FBz	248	81.4%	-3.7		
PFBz	236	98.4%	-10.2	89.4%	-4.5

Y. Jiang, T. Lee and C. Rose-Petruck, J. Phys. Chem. B 107 (2003)
T. Lee, Y. Jiang, F. Benesch and C. Rose-Petruck, SPIE 4978 (2003)

X-ray and infrared spectroscopy: Complementary methods probing molecular structure and molecular symmetry

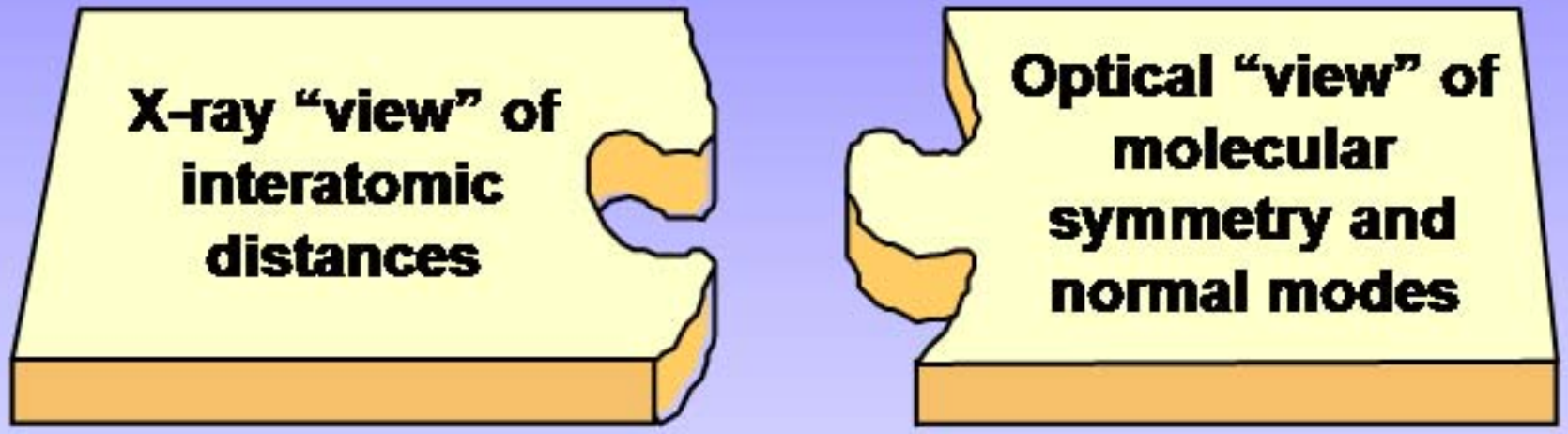

Multiple scattering paths of IPC-Bz at 0 Kelvin

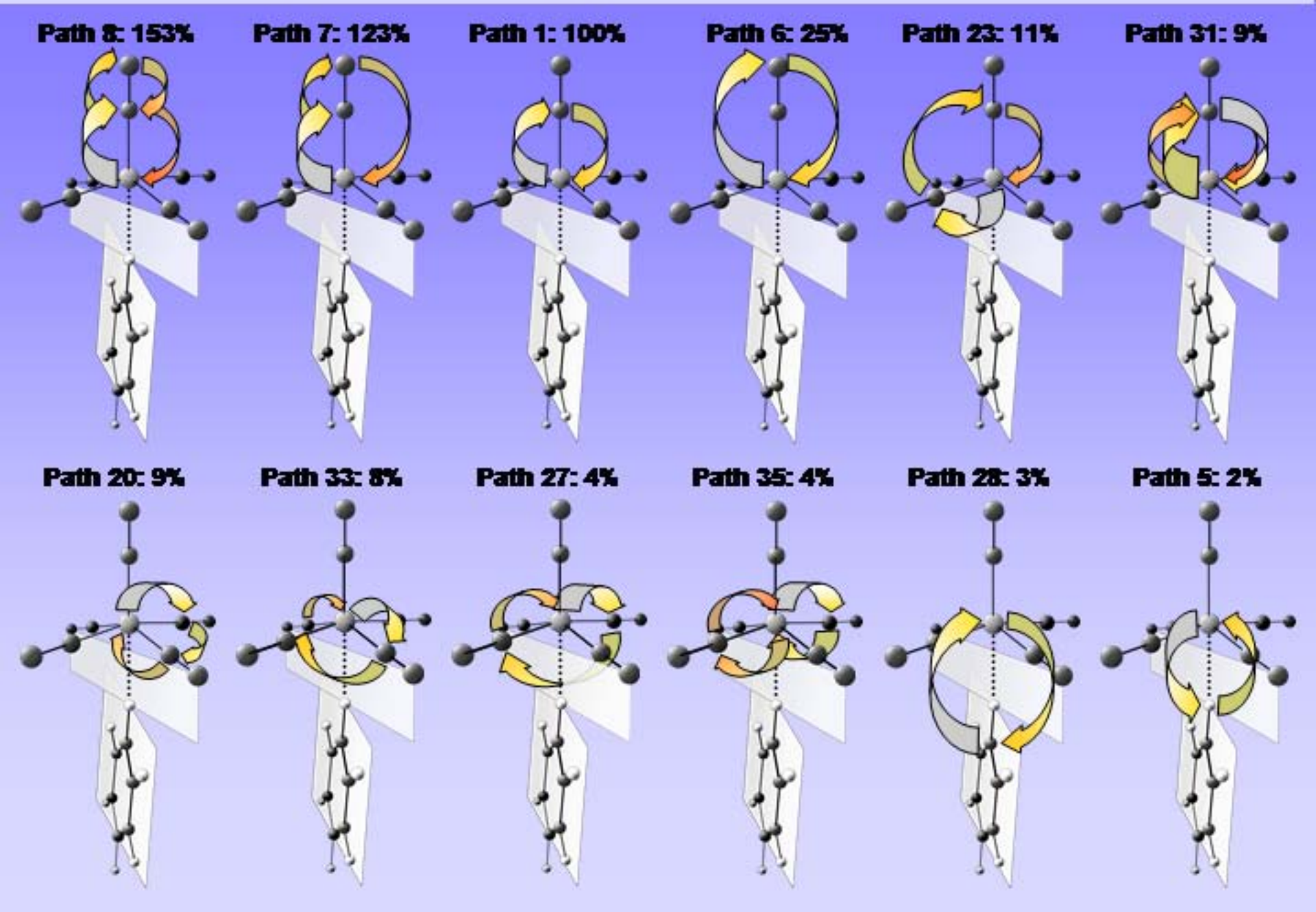

XAFS spectrometer

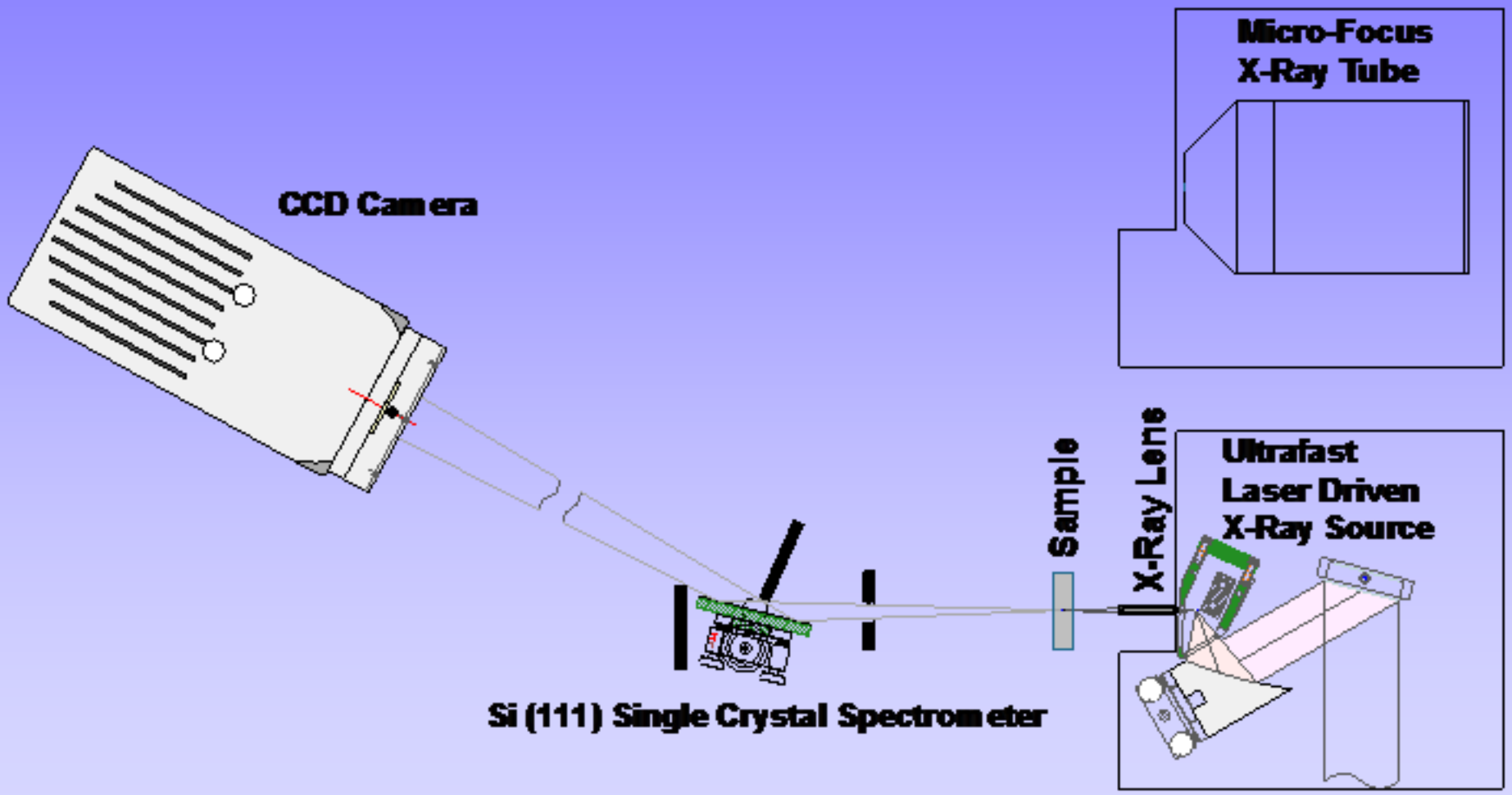

Experimental and theoretical XAFS spectra of IPC-Bz

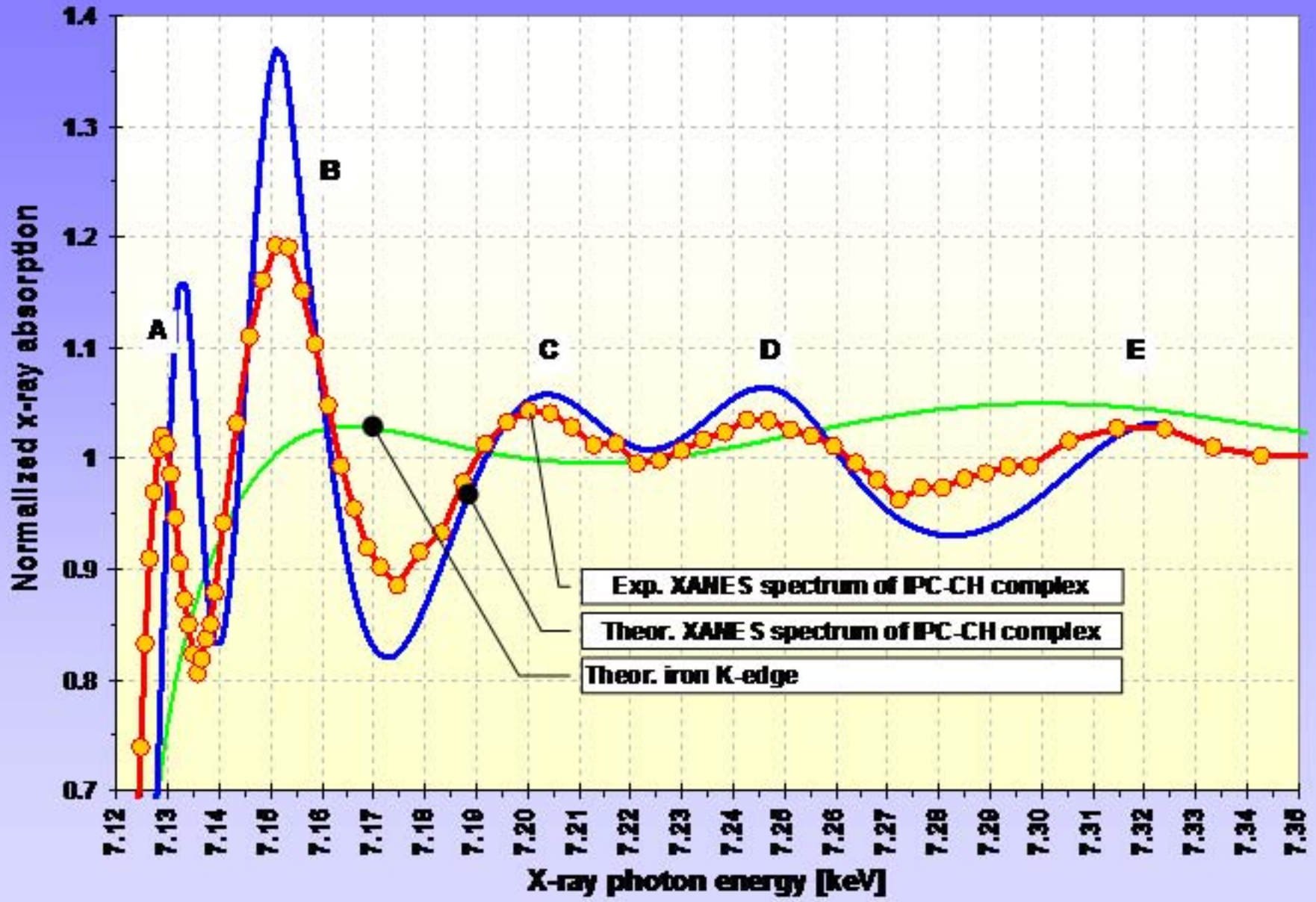

XAFS of IPC-Bz measured with laser plasma source

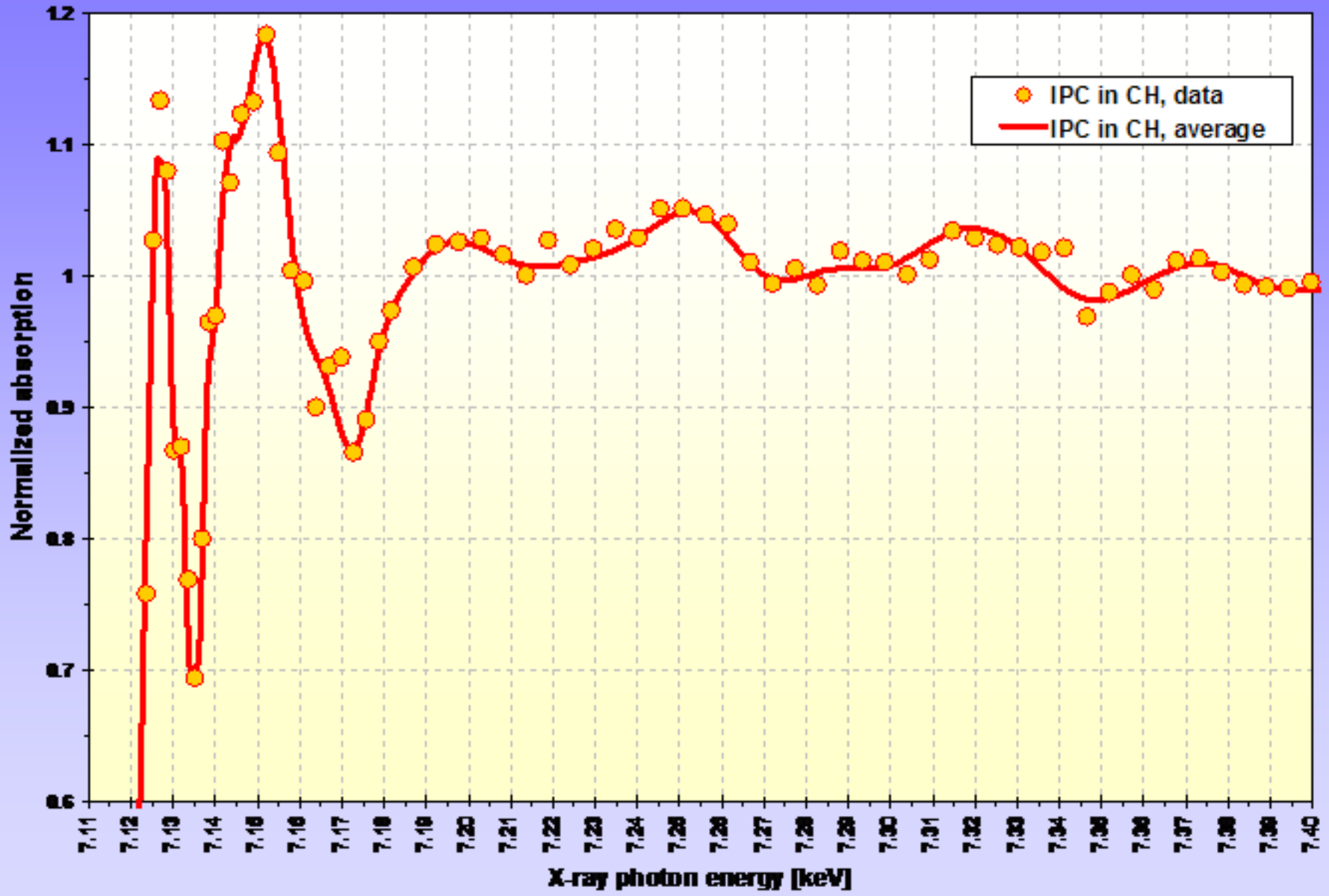

Measured XAFS of IPC-Bz and multiple-scattering fit

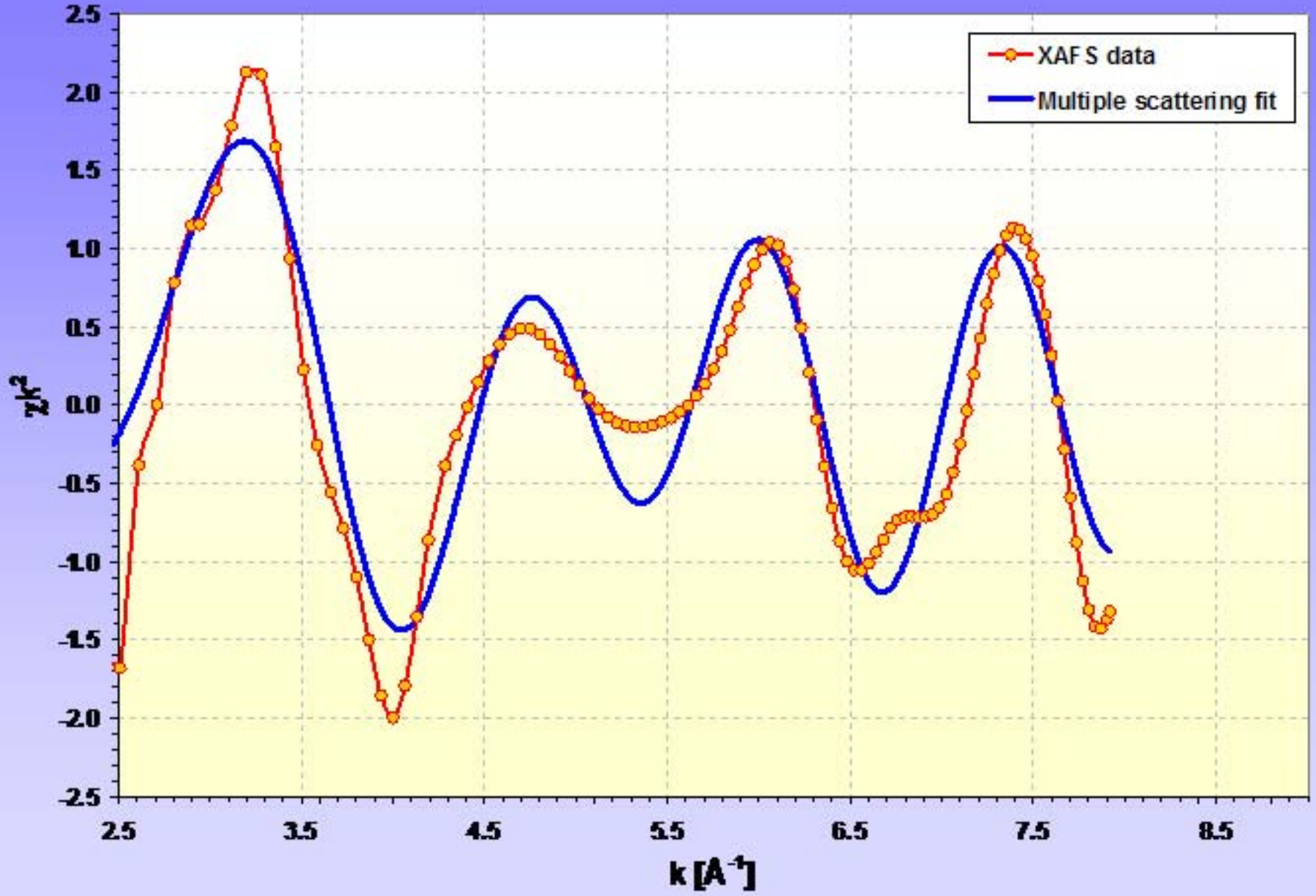

Fourier transform of measured and fitted XAFS of IPC-Bz

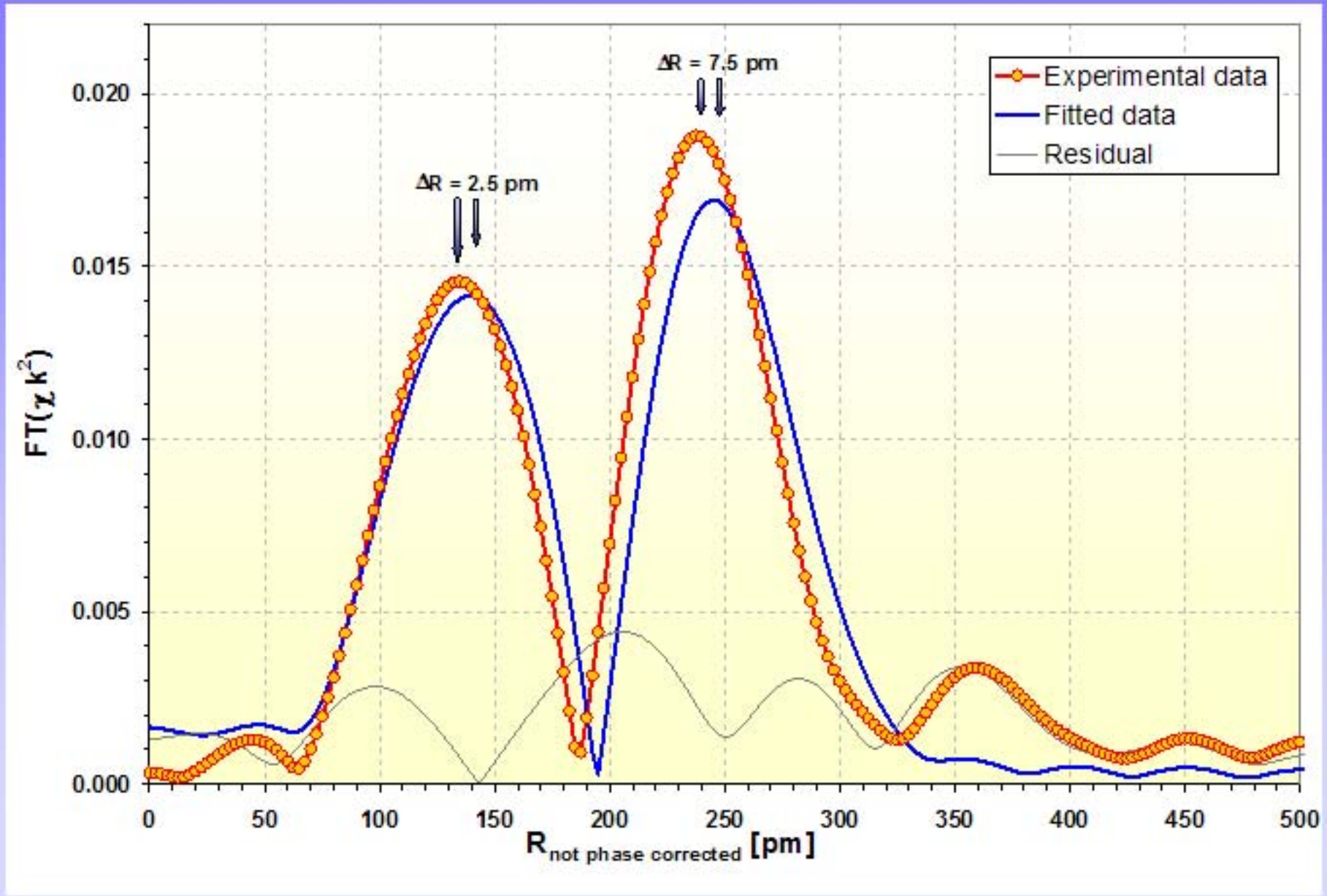

Measured XAFS of IPC-Bz and multiple-scattering fit

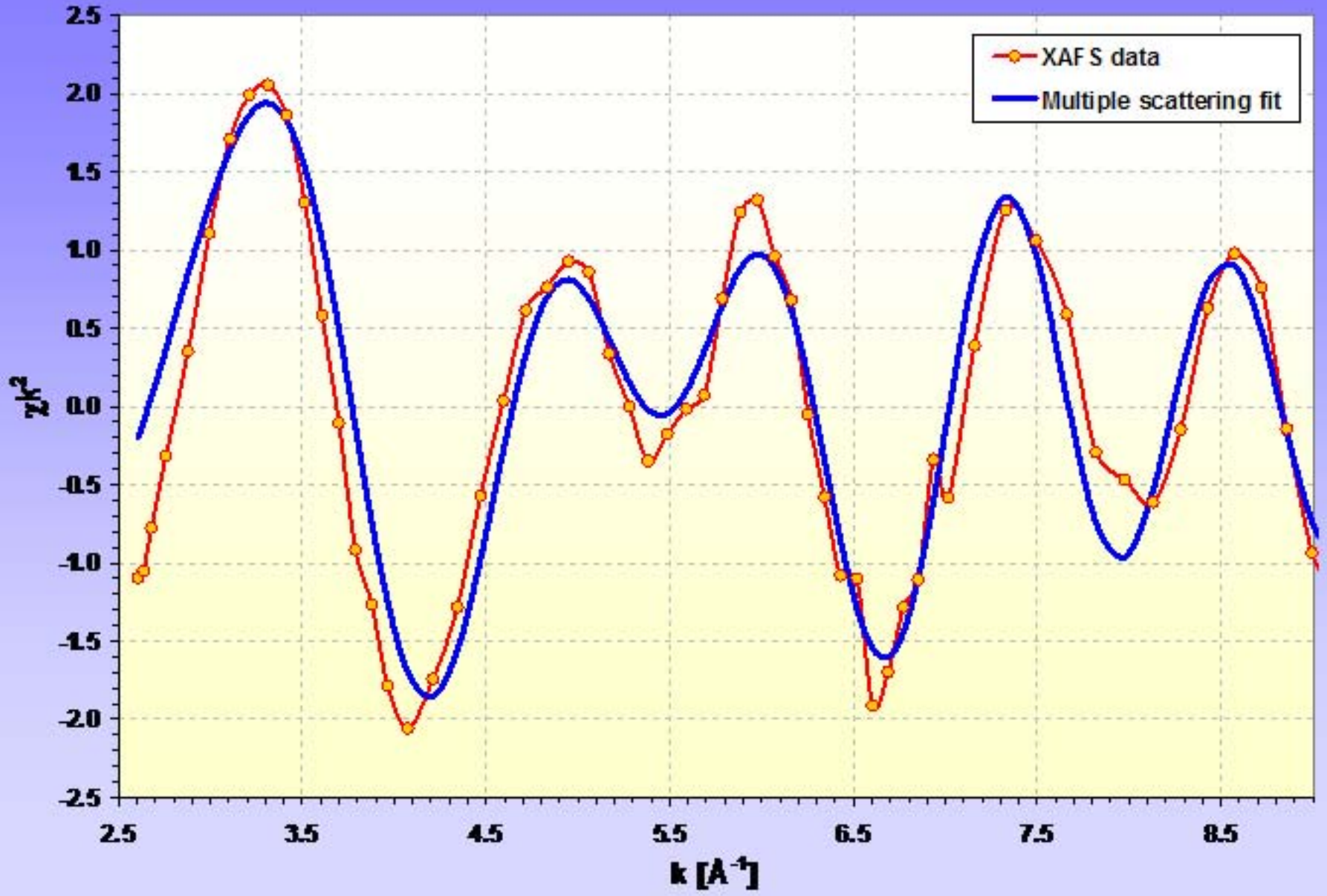

Fourier transform of measured and fitted XAFS of IPC-Bz

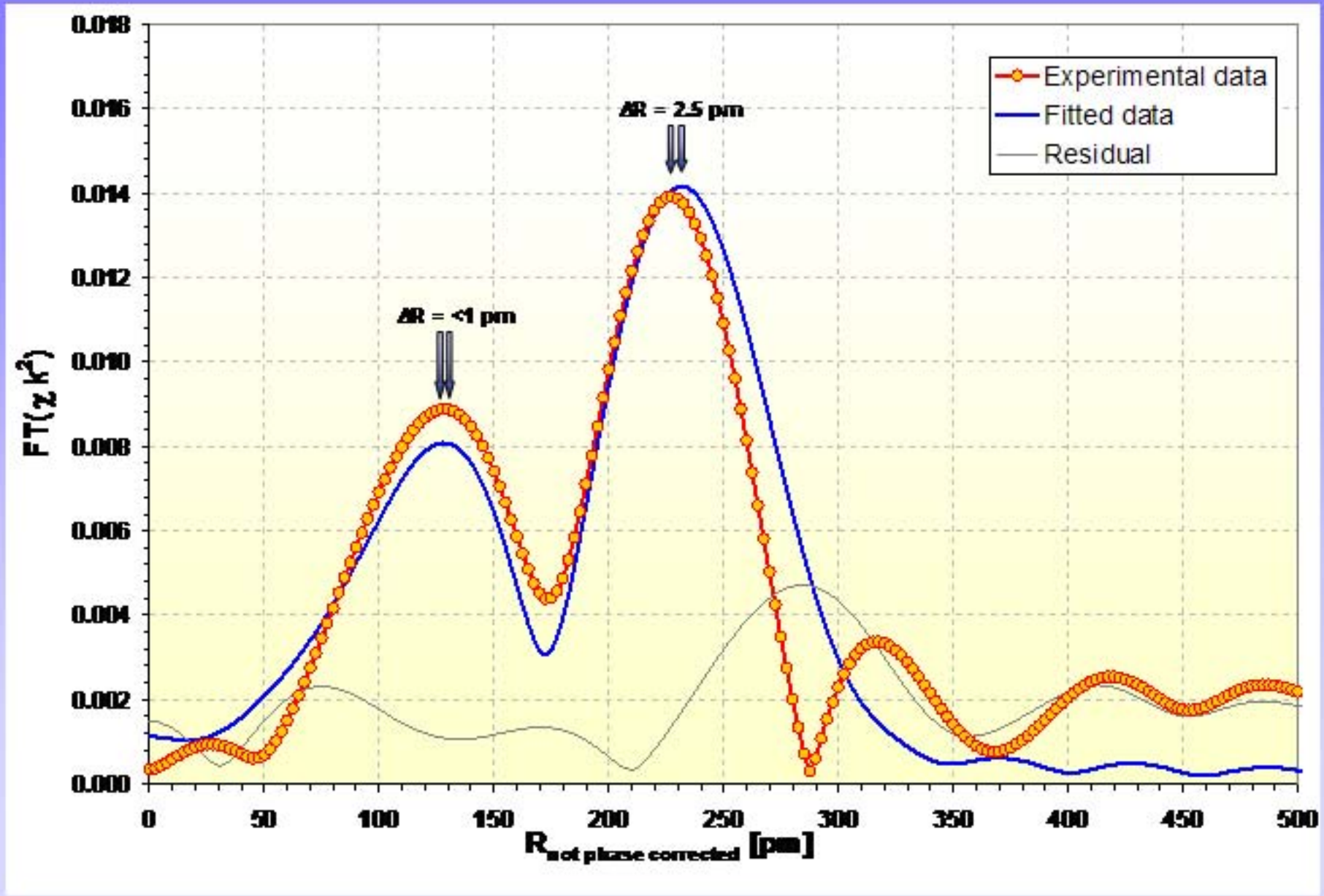

Experimental and theoretical structural data of IPC-Bz

	IPC-CH	IPC-Bz	IPC-Bz
X-ray source	Laser-driven plasma	Micro focus	DFT results
R(Fe-C) [pm]	174.2 ± 2	181.3 ± 1	181.4
R(Fe-O) [pm]	291.7 ± 6	294.4 ± 2.5	296.2
R(C-O) [pm]	117.5 3.9%	113.1 -1.5%	114.8
σ^2(Fe-C) [pm^2]	175.0	129.3	
σ^2(Fe-O) [pm^2]	15.3	57.5	
S_0^2	0.990	2.471	
E_0 [eV]	-0.7493	2.412	
Residual	0.42	0.27	

T. Lee, Y. Jiang, and C. Rose-Petruck, Chemical Physics, in press (2003)
T. Lee, Y. Jiang, F. Benesch, N. Song and C. Rose-Petruck, SPIE 5196 (2003)

Outline

- High-brightness, tabletop x-ray sources
  - High-average power lasers for x-ray generation
  - Ultrafast x-ray sources and x-ray optics
- Structural deformations of solvated $Fe(CO)_5$
  - Density Functional Theory Calculations
  - FTIR measurements and conformer distribution
  - XAFS measurements and molecular structure
- **Ultrafast XANES**
  - **Expected ligand substitution dynamics of $Fe(CO)_5$**
  - **UXAFS features of $Fe(CN)_5^{4-}$**
  - **Example: Simulation of ultrafast x-ray diffraction**
- Future performances of laser plasma sources

Possible photoinduced ligand substitution

1. $(OC)_5Fe\cdots H$

$+ h\nu\ (\lambda \geq 400\ nm)$

2. $(OC)_4Fe$ $+ CO$

3. $(OC)_4Fe$ 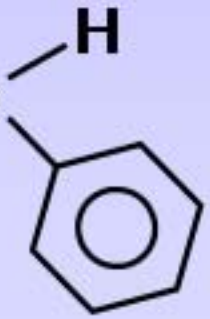 $+ CO$

Theoretical XANES spectra for ligand substitution and dissociation

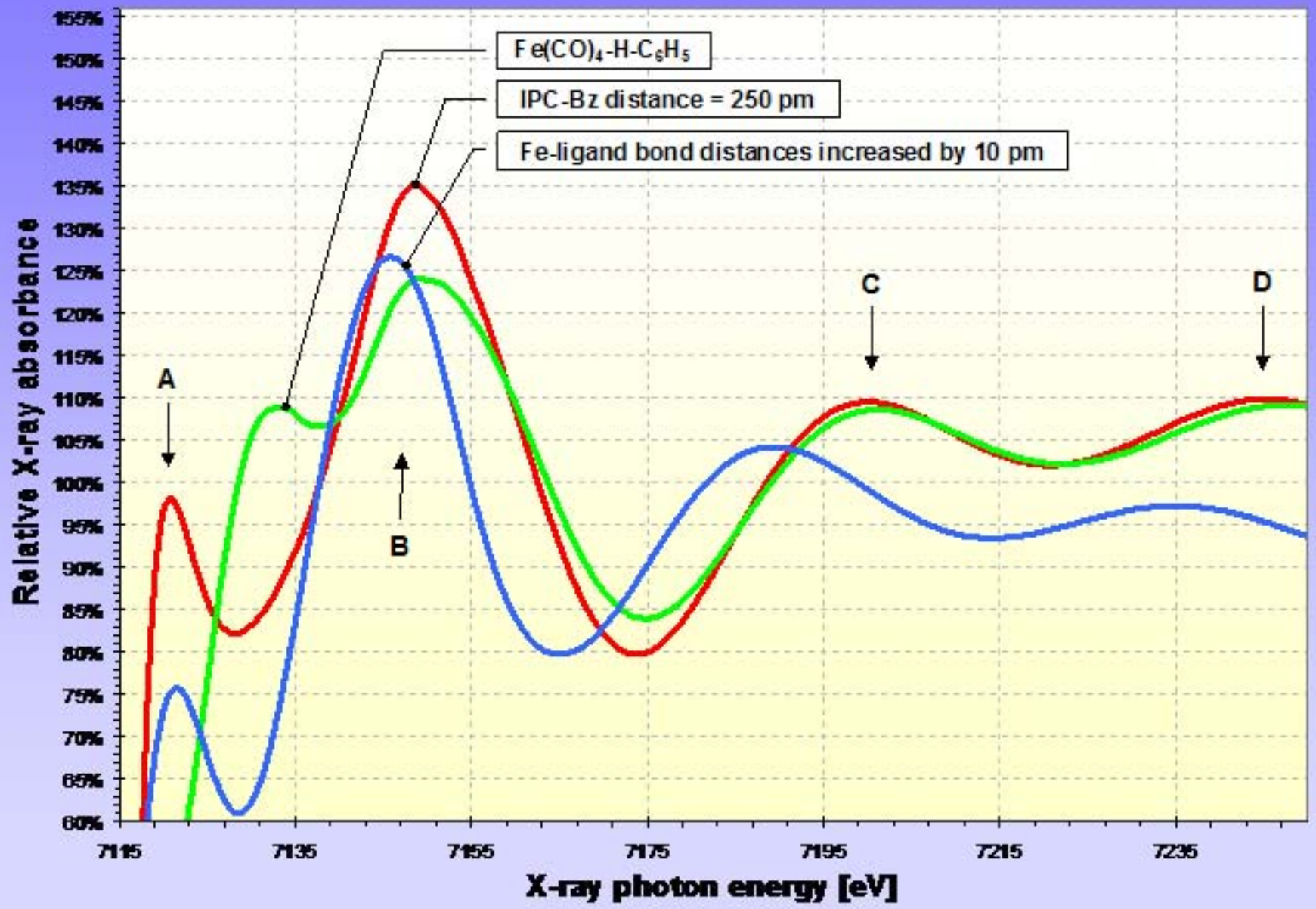

Currently in the spectrometer ….
Excited state chemistry of iron hexacyanide in water

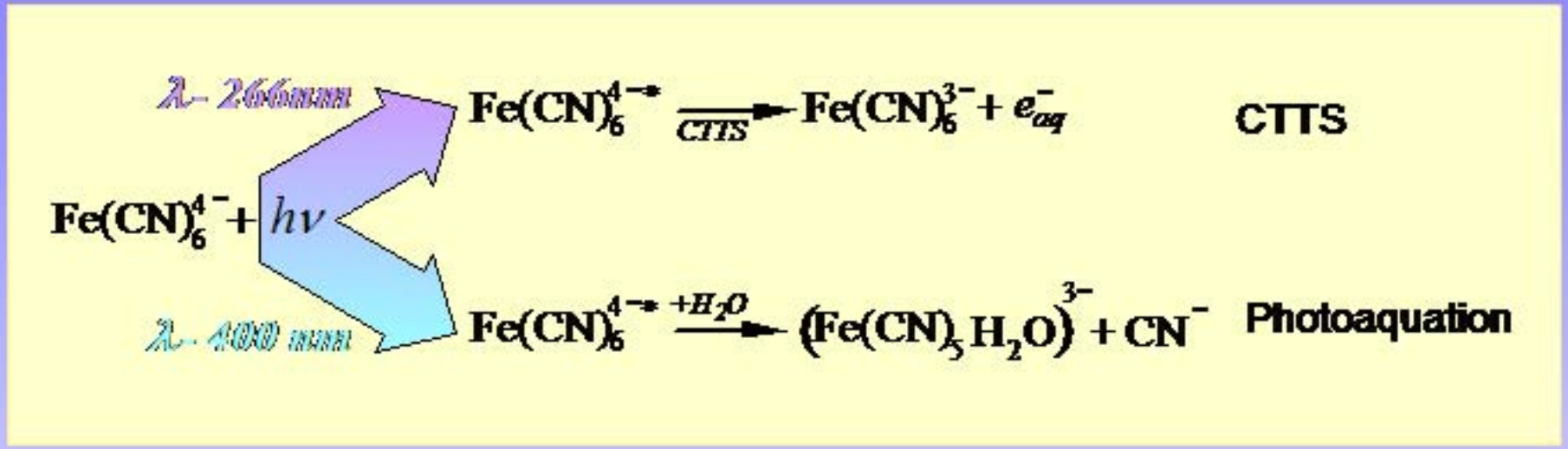

- Excitation photon wavelength < 270 nm: Charge Transfer To Solvent
- Excitation photon wavelength < 400 nm: Photoaquation

XANES measurements of $Fe(CN)_6^{3-}$ and $Fe(CN)_6^{4-}$ in water

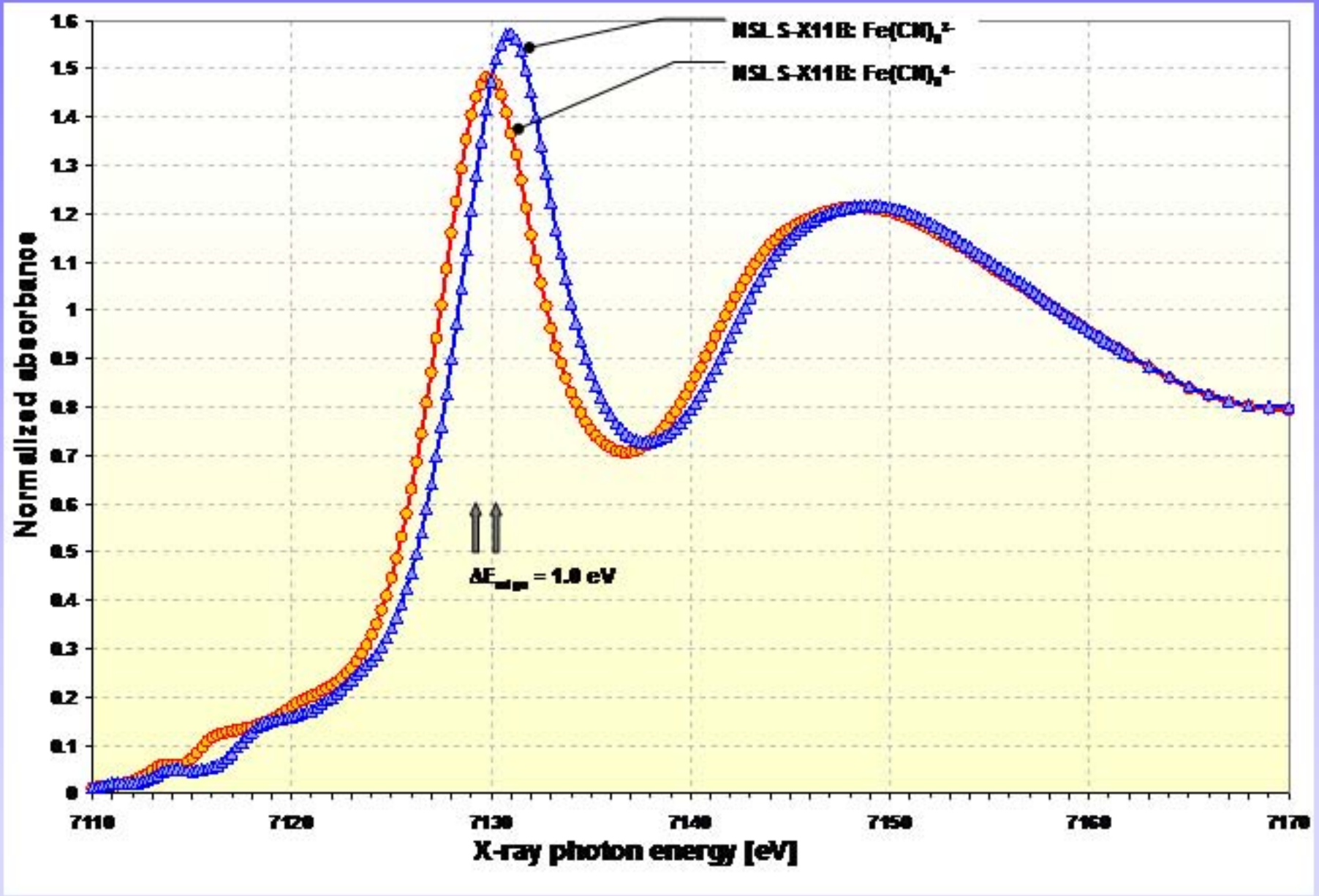

EXAFS measurements of $Fe(CN)_6^{3-}$ and $Fe(CN)_6^{4-}$ in water

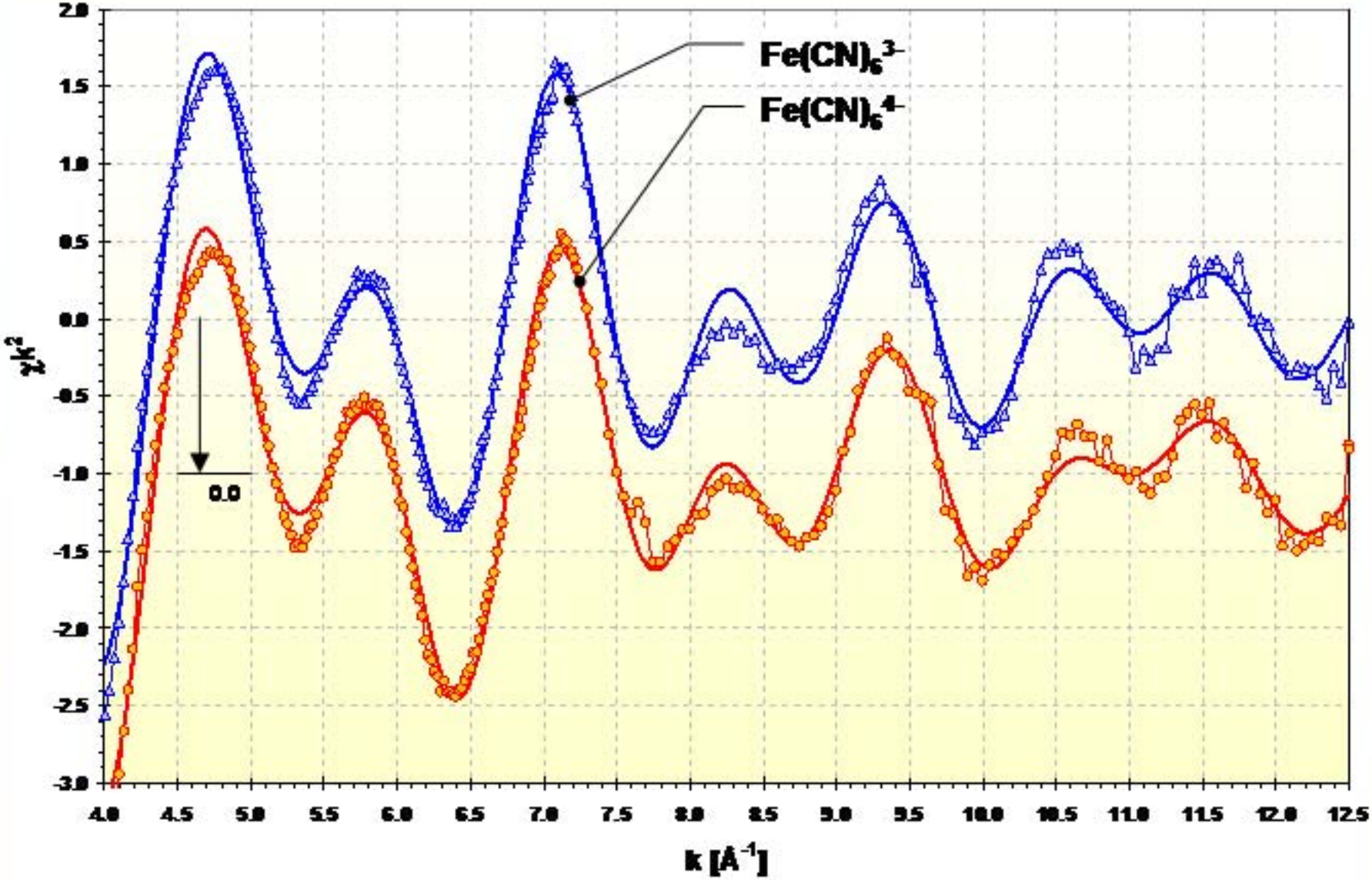

Radial distribution function of $Fe(CN)_6^{3-}$ and $Fe(CN)_6^{4-}$ in water

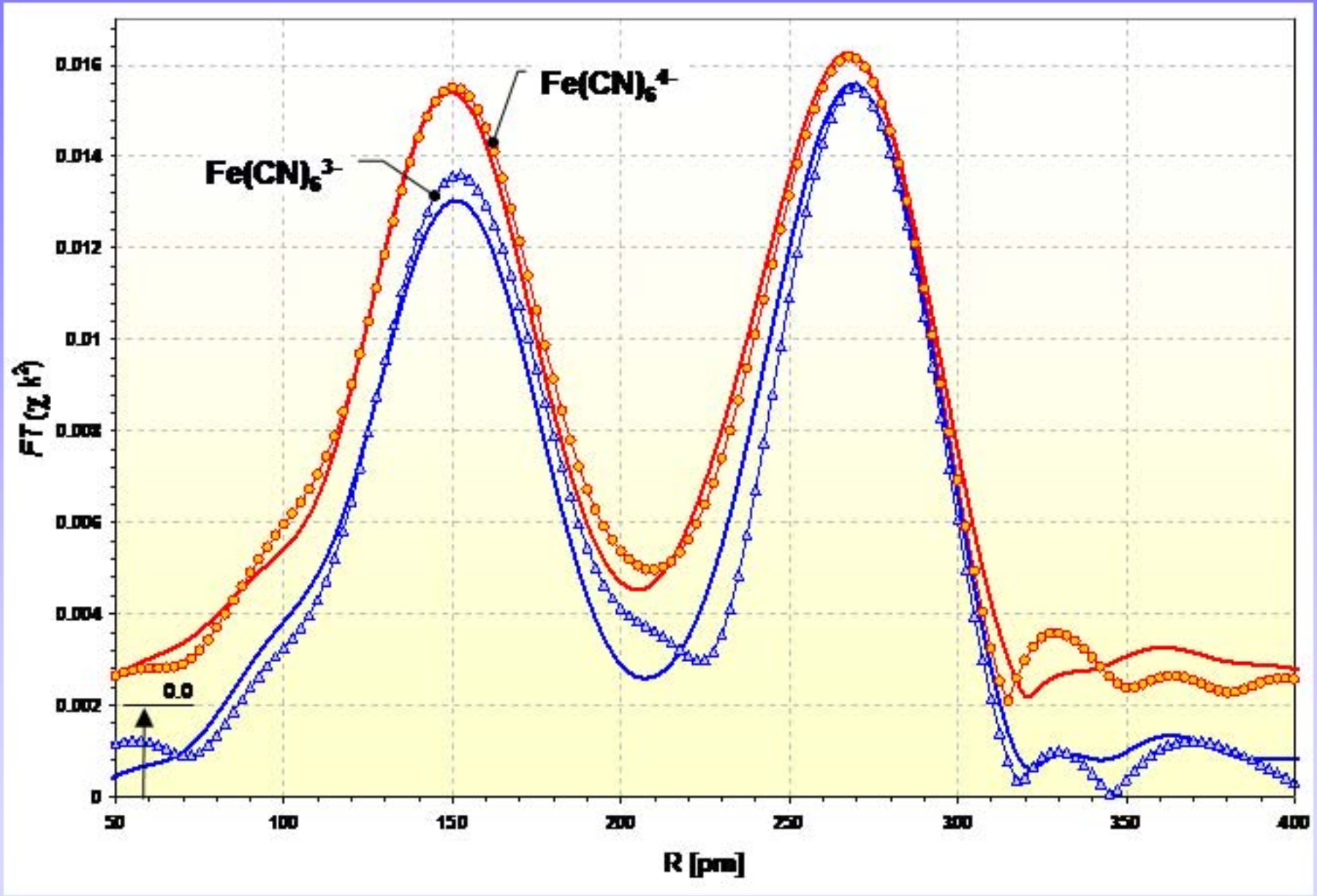

Structural parameters of $Fe(CN)_6^{3-}$ and $Fe(CN)_6^{4-}$ in water

X-ray source	NSLS			DFT results		
parameter	$[Fe^{II}(CN)_6]^{4-}$	$[Fe^{III}(CN)_6]^{3-}$	Differences Fe^{III} - Fe^{II}	$[Fe^{II}(CN)_6]^{4-}$	$[Fe^{III}(CN)_6]^{3-}$	Differences Fe^{III} - Fe^{II}
R(Fe-C) [pm] (fit)	187.6 ± 0.2	190.1 ± 0.2	2.5 ± 0.3	202.9	199.5	-3.5
R(Fe-N) [pm] (fit)	308.8 ± 0.8	309.7 ± 0.6	0.9 ± 1.0	321.2	316.9	-4.4
R(C-N) [pm] (calcul.)	121.1 ± 0.8	119.6 ± 0.7	-1.5 ± 1.0	118.3	117.4	-0.9
s^2(Fe-C) [pm^2] (fit)	25.4 ± 3.5	46.3 ± 4.4	20.9 ± 5.6			
s^2(Fe-N) [pm^2] (fit)	53.9 ± 3.7	37.5 ± 3.3	-16.4 ± 5.0			
Coordination #:						
Fe-C and Fe-N (fit)	4.9 ± 0.2	6.6 ± 0.3	1.7 ± 0.3			
Fe-C-N (fit)	12 ± 0.6	12 ± 0.6	-0.4 ± 0.9			
Fe-C-N-C (fit)	0.1 + 0.8	0.7 + 0.7	0.6 ± 1.1			
E_0 [eV] (fit)	-3.9 ± 0.4	-2.9 ± 0.4	1.0 ± 0.5			
S_0^2 (fixed)	1.00	1.00				
Residual	15.4%	16.6%				
K-edge position [eV]	7127.75	7128.75	1.0			

Ultrafast laser-driven XAFS spectrometer

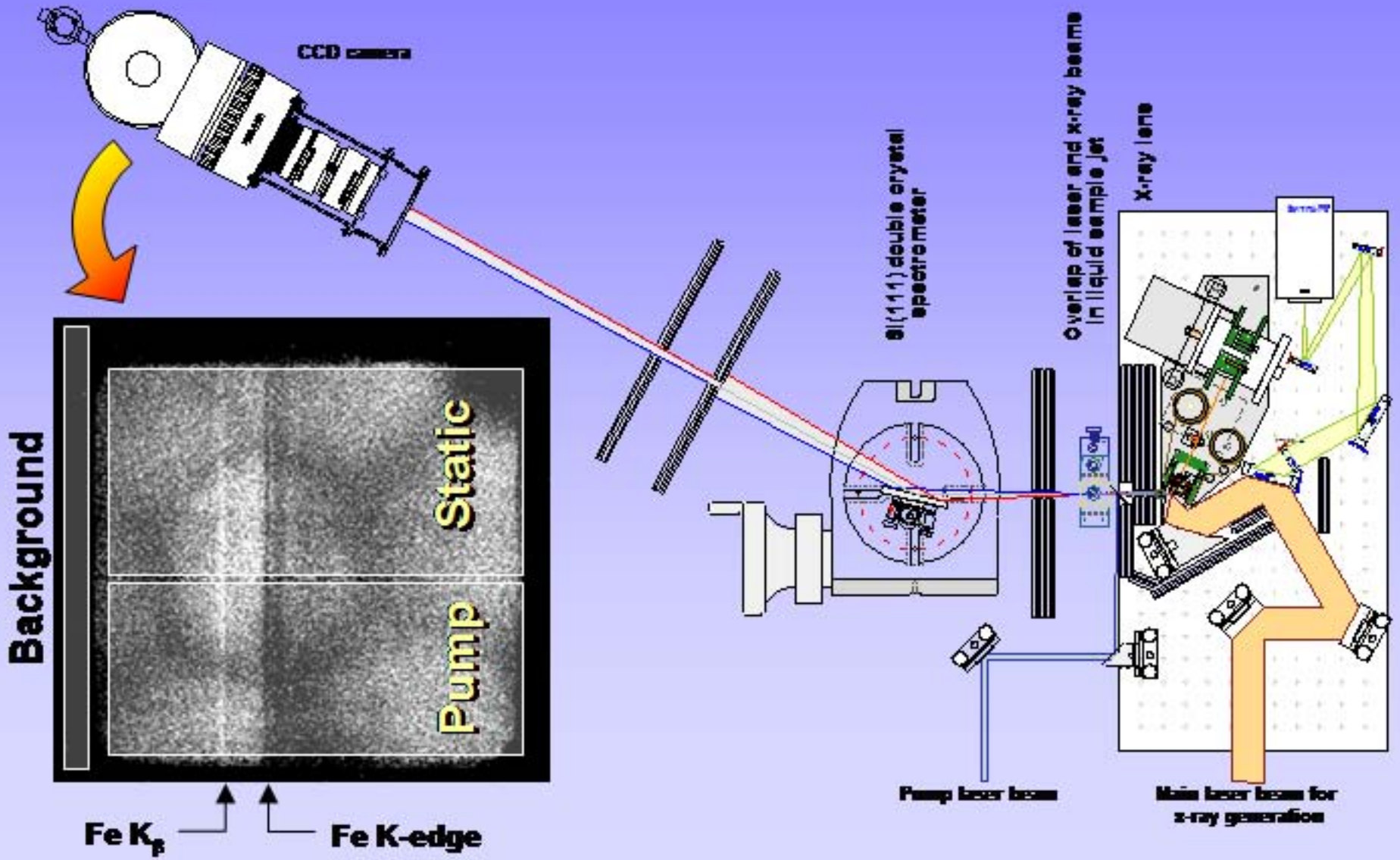

UXANES at –30 ps, 0 ps, and +40 ps after photoexcitation

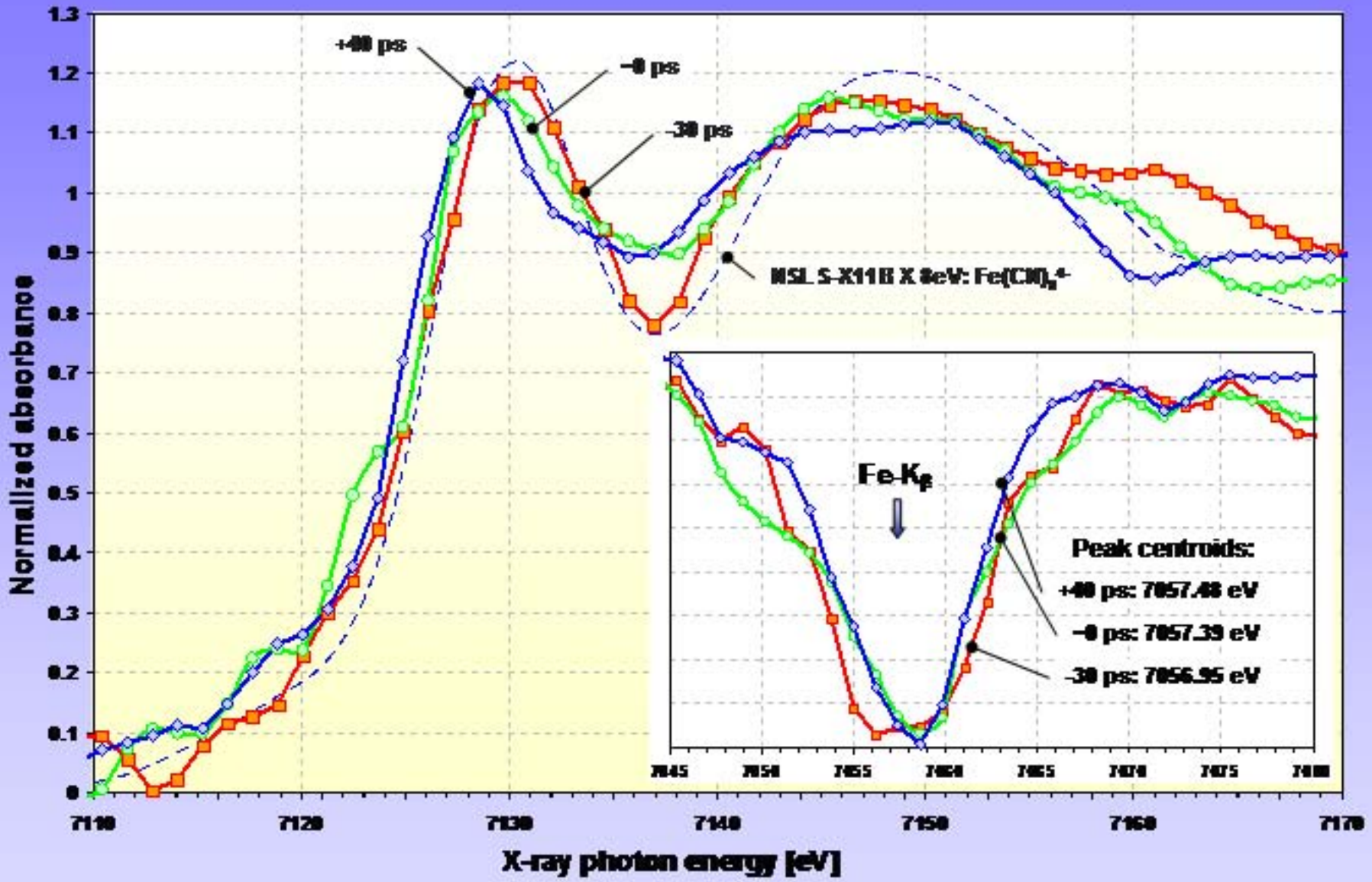

Radial Fe-ligand bond lengths increase of $Fe(CN)_6^{4-}$

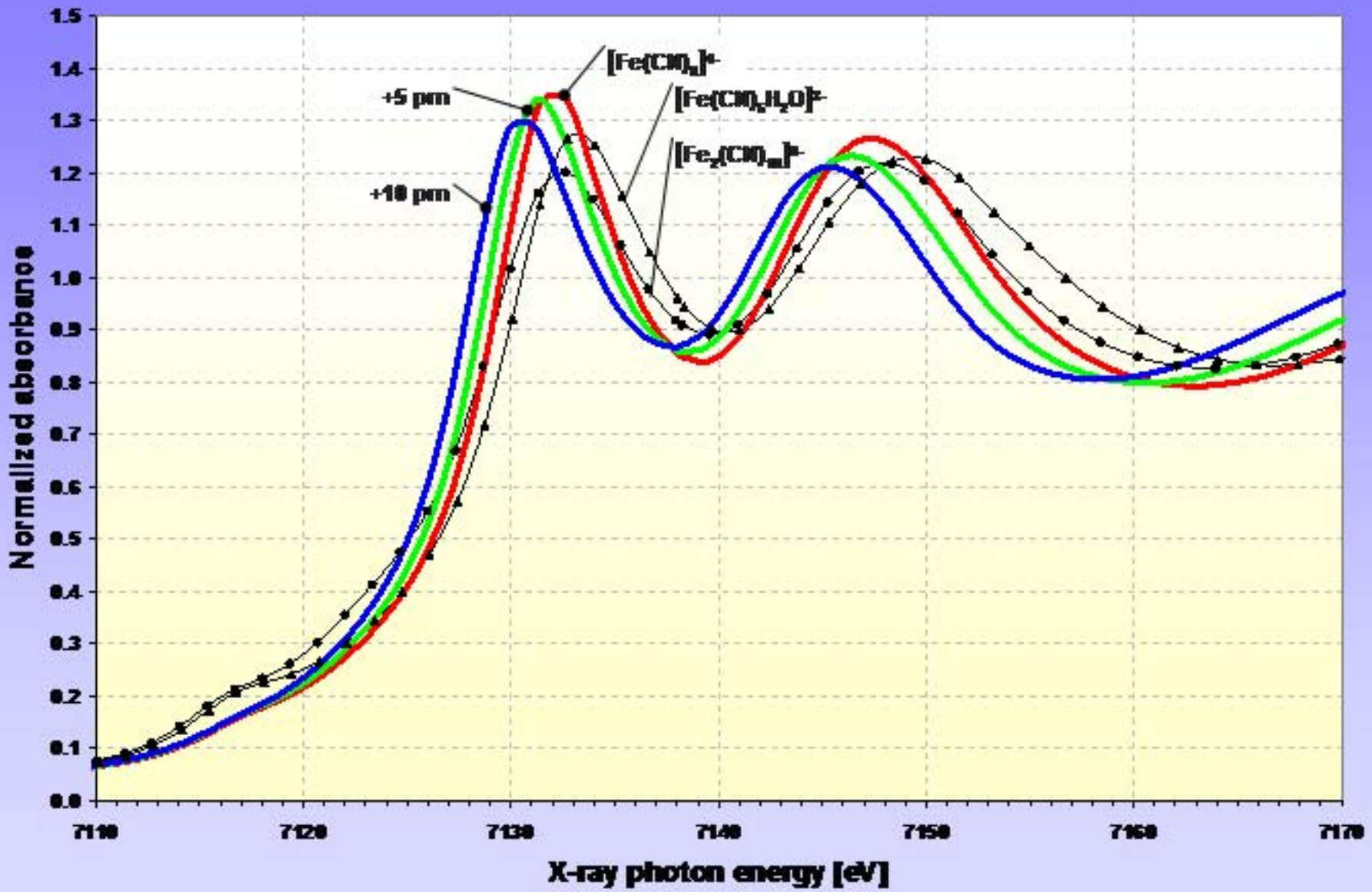

Simulation of ultrafast x-ray diffraction

The I_2-reflectron

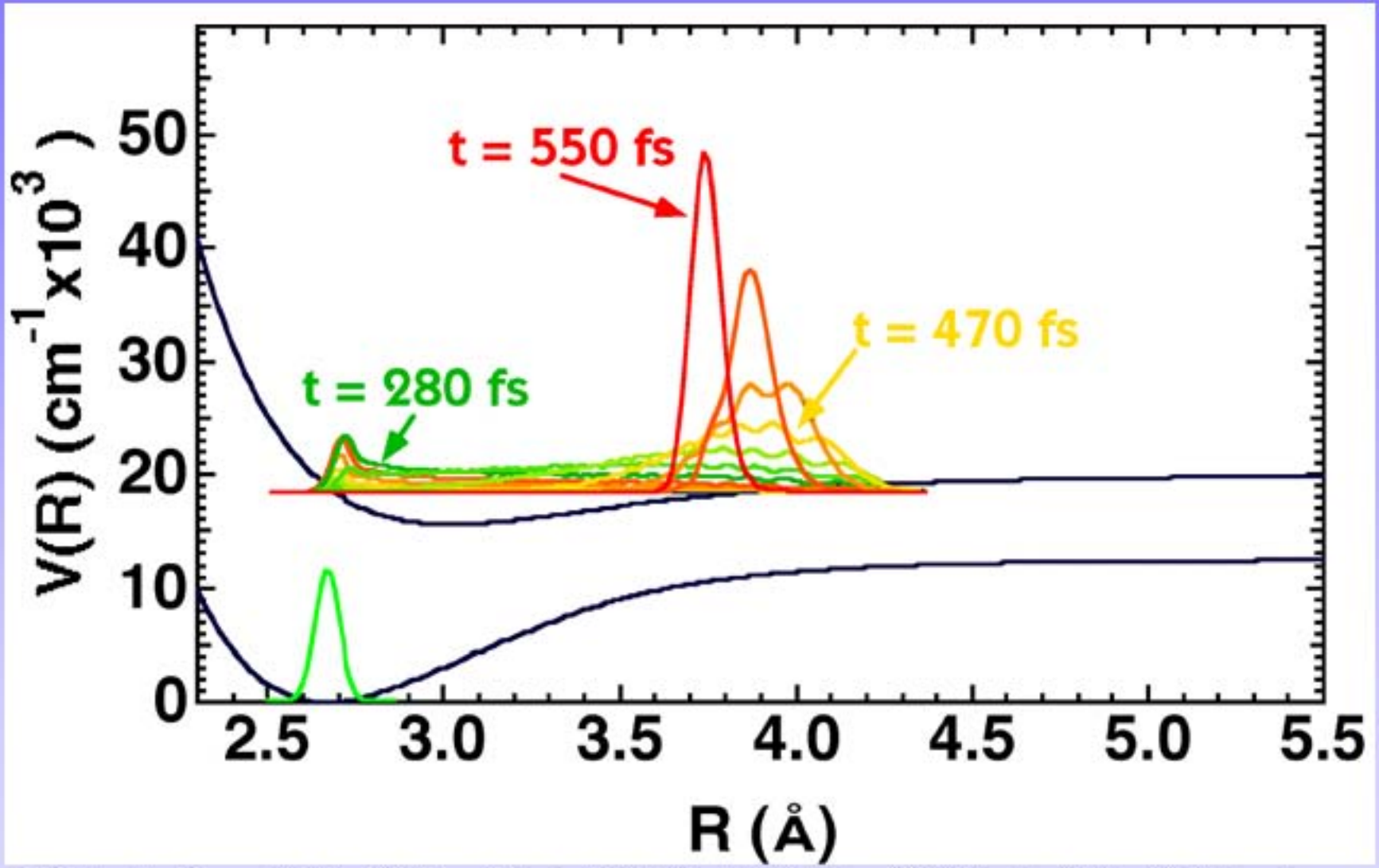

B. Kohler, J.L. Krause, F. Ráksi, C. Rose-Petruck, R.M. Whitnell, K.R. Wilson, V.V. Yakovlev, Y. Yan, S. Mukamel, *J. Phys. Chem.* **97**, 12602 (1993)

I-I distance probability distributions

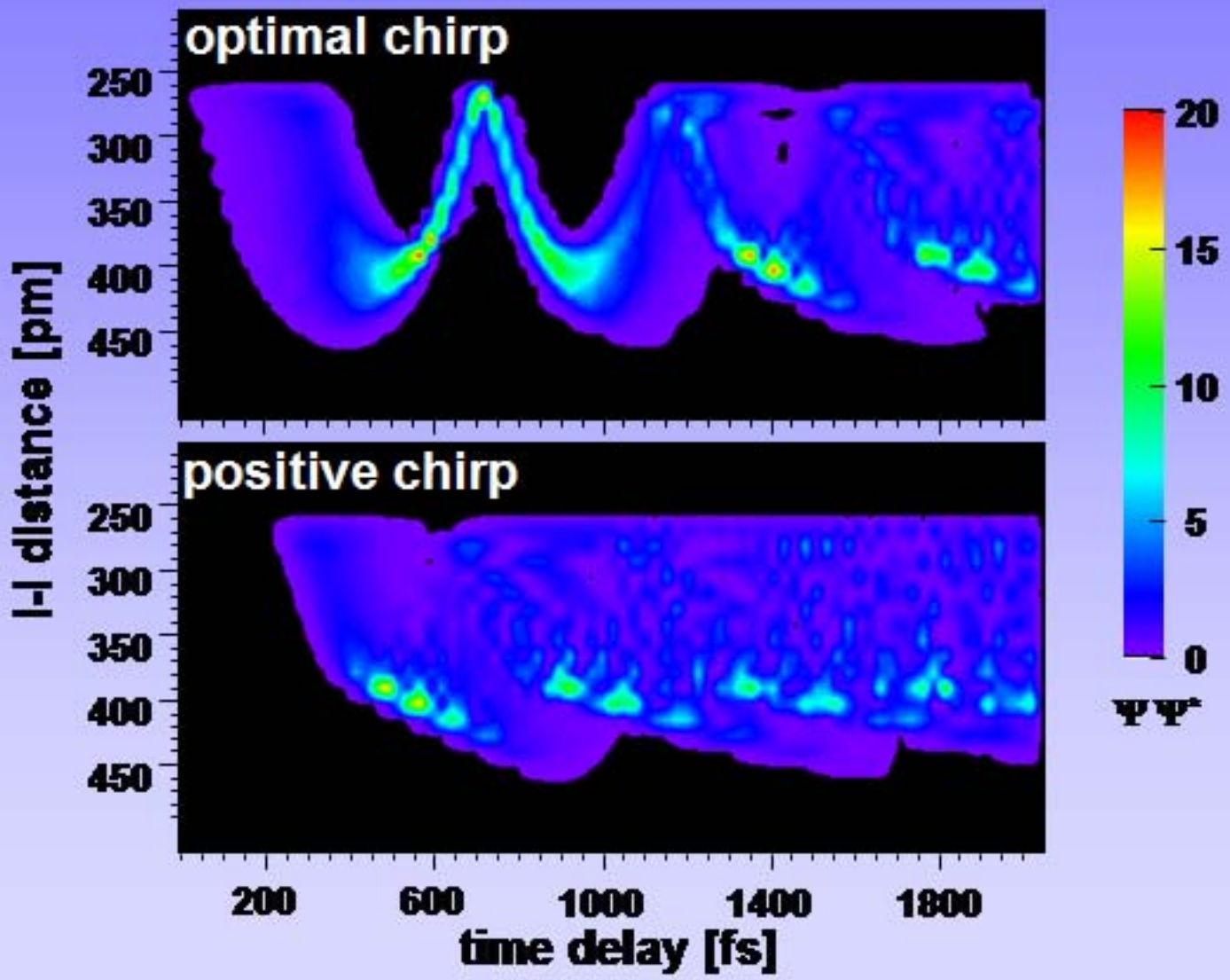

Simulated diffraction pattern for Cu-K_α x-ray pulses

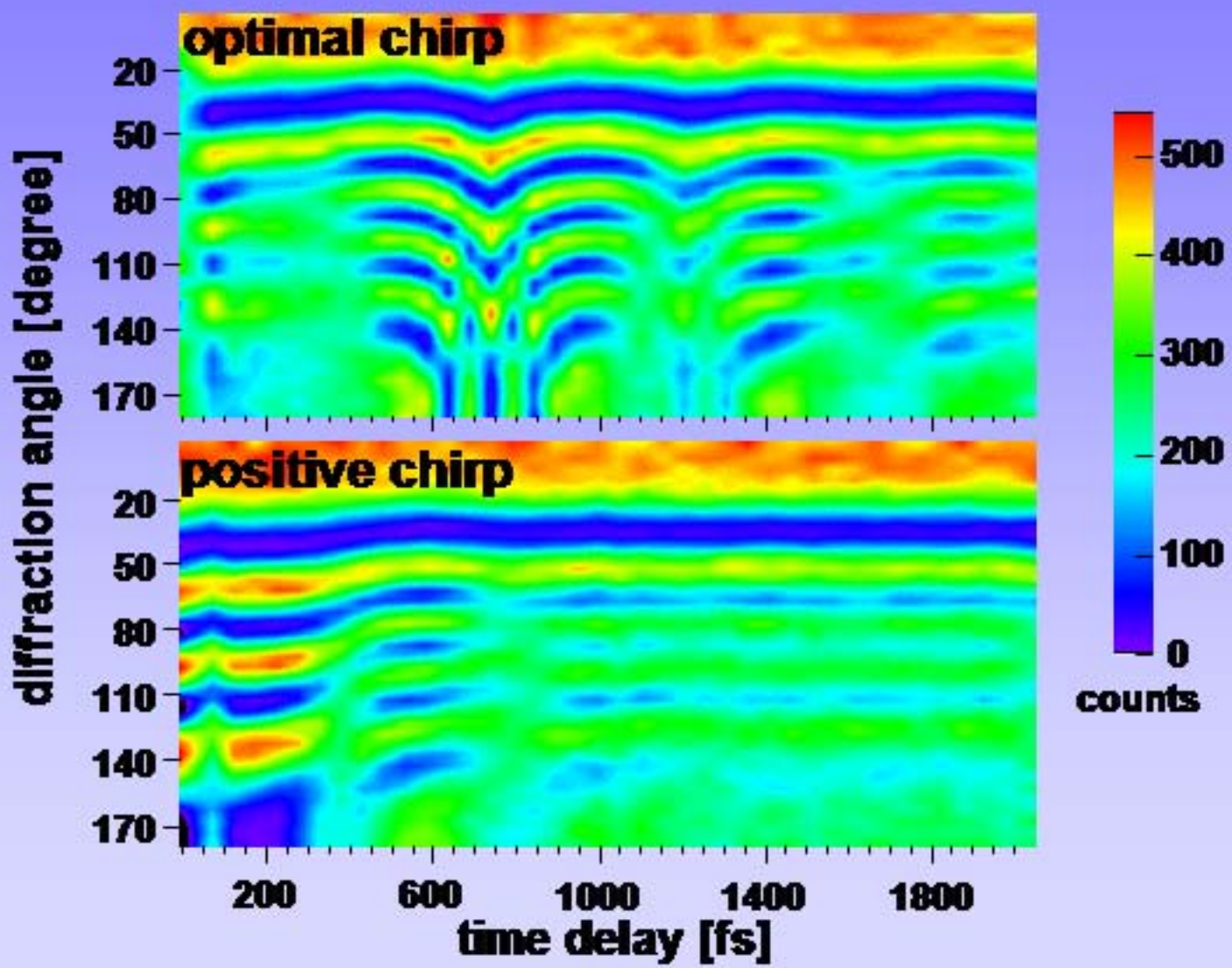

Nuclear motions and ultrafast x-ray diffraction off I_2

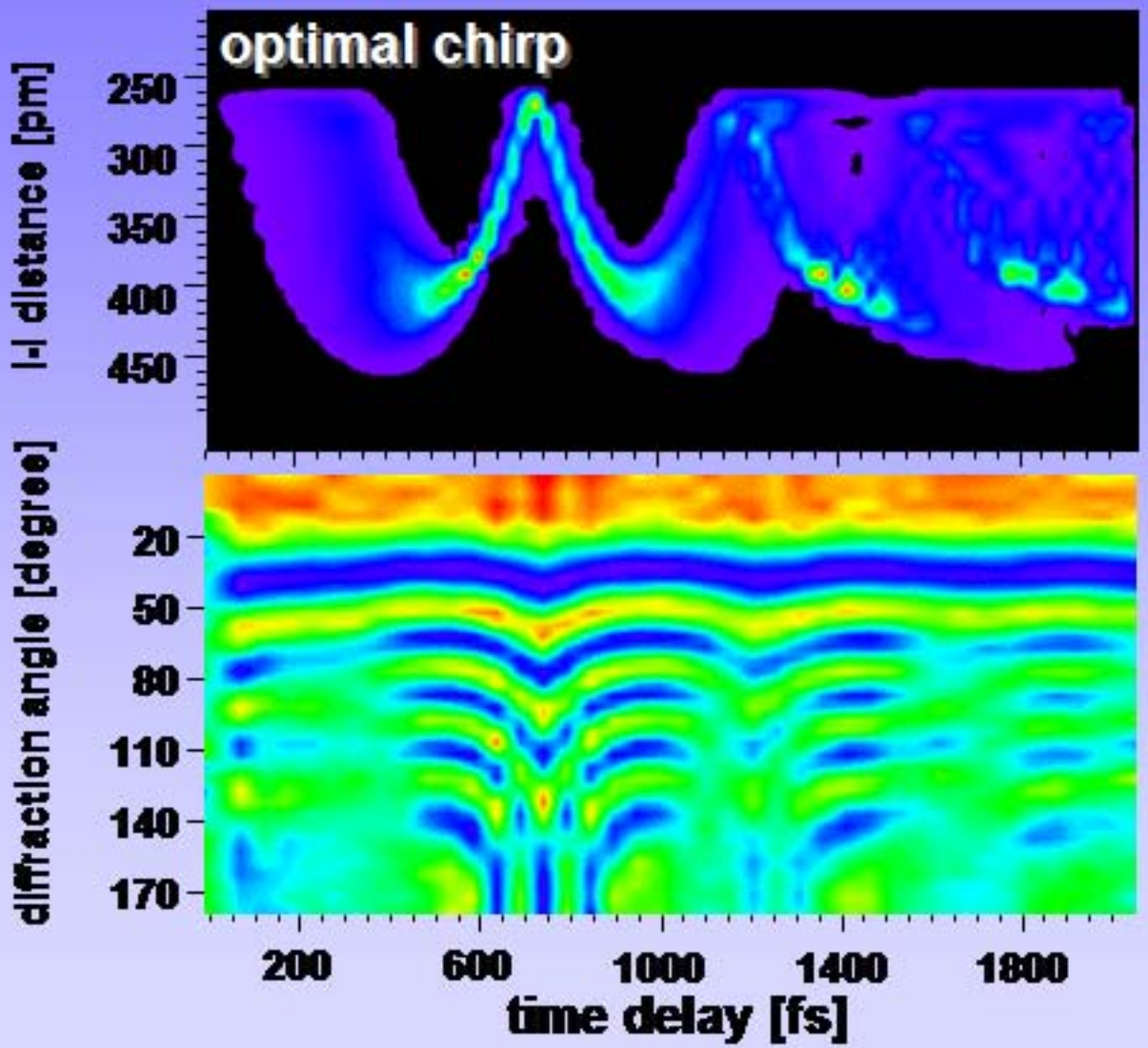

Outline

- High-brightness, tabletop x-ray sources
  - High-average power lasers for x-ray generation
  - Ultrafast x-ray sources and x-ray optics
- Structural deformations of solvated $Fe(CO)_5$
  - Density Functional Theory Calculations
  - FTIR measurements and conformer distribution
  - XAFS measurements and molecular structure
- Ultrafast XANES
  - Expected ligand substitution dynamics of $Fe(CO)_5$
  - UXAFS features of $Fe(CN)_6^{4-}$
  - Example: Simulation of ultrafast x-ray diffraction
- **Future performances of laser plasma sources**

Comparison of laboratory-based hard x-ray sources

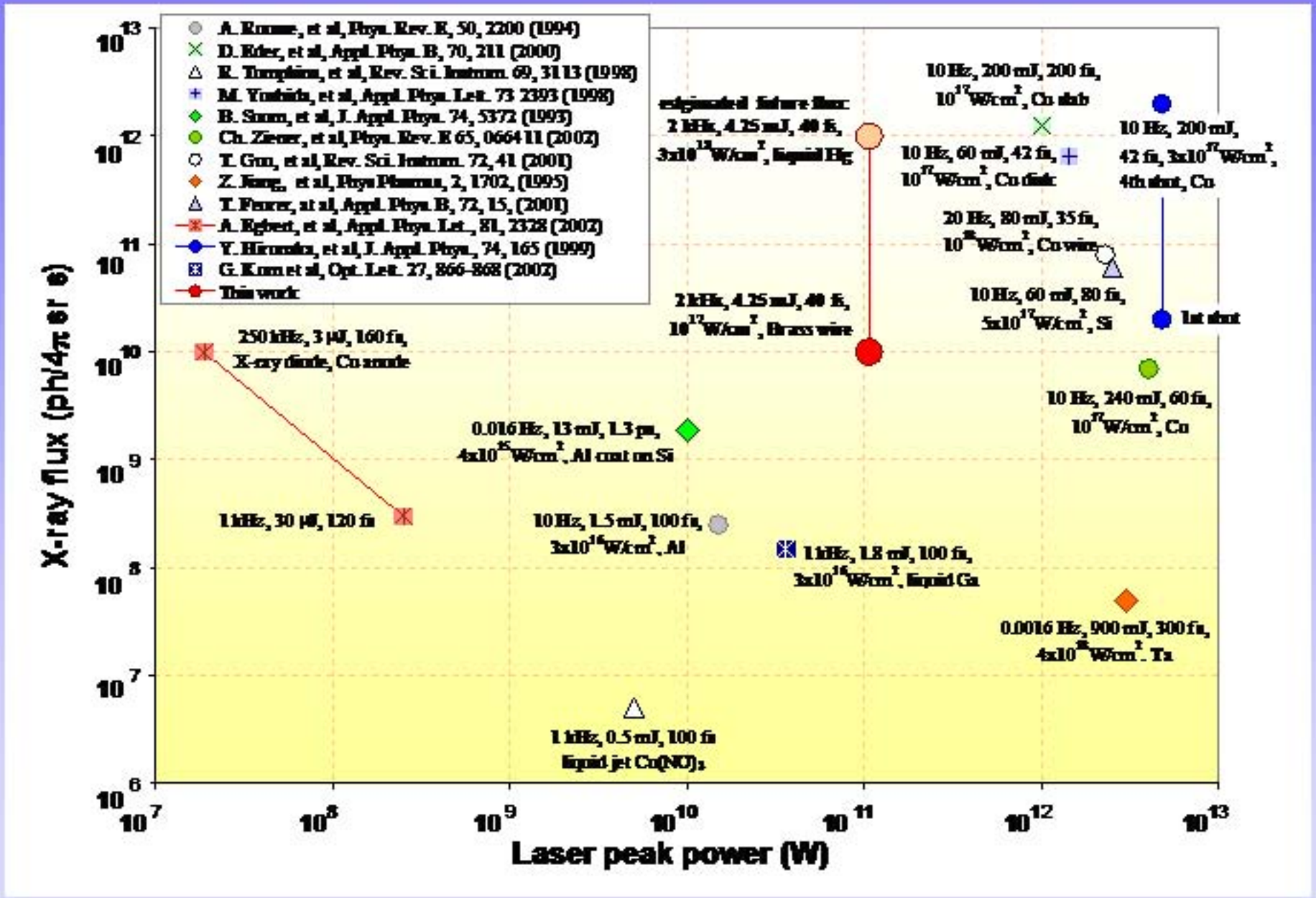

Ultrafast fiber lasers for laser-driven x-ray sources?

Average power of up to 5.5W at 1 MHz pulse-repetition rate.

June 15, 2001 / Vol. 26, No. 12 / OPTICS LETTERS 935

Generation of high-energy femtosecond pulses in multimode-core Yb-fiber chirped-pulse amplification systems

A. Galvanauskas, G. C. Cho, A. Hariharan, M. E. Fermann, and D. Harter

IMRA America, Inc., 1044 Woodridge Avenue, Ann Arbor, Michigan 48105-9774

Received December 14, 2000

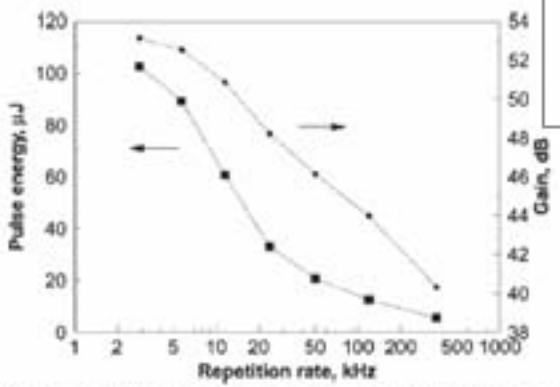

Fig. 3. Measured double-pass gain and output energy as a function of pulse-repetition rate for a double-pass Yb-fiber amplifier.

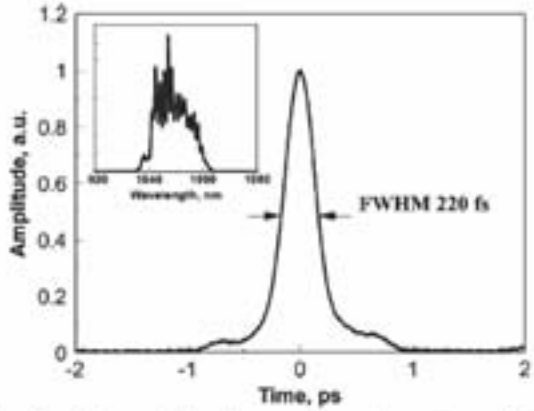

Fig. 4. Autocorrelation trace and spectrum of amplified recompressed pulses.

High power fiber lasers.

A.Galvanauskas. Optical Sciences Laboratory, Center for Ultrafast Optical Science, Univ. of Michigan, Ann Arbor,

Optics & Photonics News (2004), 15(7), 42-47.

Abstract

Recent advances in fiber and laser diode technologies have led to kilowatt-power fiber lasers with output beams of single transverse mode quality. Considering the significant practical advantages of optical fibers, this development is likely to profoundly affect laser technol. and stimulate the use of lasers in a range of practical applications.

Scaling of laser plasma sources

	Factor	Flux [ph / 1keV s]	Data acquisition time per delay step
Currently detected flux		50	24 h
Crystal imaging optics	100	5000	17.28 s
Liquid metal source	100	500000	0.1728 s
Laser power upgrade (from 6 W to 20 W on target)	4	2.E+06	43.2 ms
Future fiber lasers, 10 kW, 1MHz (10 mJ / pulse)	500	1.E+09	86.4 us

Summary

- Previously unrecognized solvation structure of penta-coordinated complexes: Solvated $Fe(CO)_5$ mostly C_{4v}, C_{2v}
  - Mechanistic consequence: Concerted ligand substitution possible
  - UF-dynamics consequence: Coherence transfer from reactant to product seems possible, $Fe(CO)_5$Solv ultrafast bi-molecular reaction system
- First system to produce usable kilohertz hard x-ray flux: about 10^{10} ph / s 4π keV at 8 keV
- First structural XAFS measurements with the laser plasma source: few pm accuracy
- First observation of picosecond structural dynamics of solvated molecules ($Fe(CN)_6^{4-}$)
- Next 2 years: Increase of detected x-ray flux: 10^4 - 10^6

Acknowledgments:

Dr. Yan Jiang
Taewoo Lee
Frank Benesch
Daniel Kuntze
Emma Welch

Dr. Claude Bailat
Theron Hamilton
Prof. Gerald Diebold

SPPS:
Dr. Peter Siddons
Dr. Chi-Chang Kao
Prof. Steven Dierker

Postdoc position open in
ultrafast X-ray Absorption Spectroscopy

Funding

National Science Foundation

Department of Energy

Army

Andrew W. Mellon Foundation

Brown University

Research Corporation

---

www.rosepetruck.chem.brown.edu